

# **SANDIA REPORT**

SAND2016-0706 Unlimited Release  
January, 2016

## **Metal-Organic Framework Thin Films as Stationary Phases in Microfabricated Gas-Chromatography Columns**

Douglas H. Read and Colin H. Sillerud

Prepared by  
Sandia National Laboratories  
Albuquerque, New Mexico 87185 and Livermore, California 94550

Sandia National Laboratories is a multi-program laboratory managed and operated by Sandia Corporation, a wholly owned subsidiary of Lockheed Martin Corporation, for the U.S. Department of Energy's National Nuclear Security Administration under contract DE-AC04-94AL85000.

Approved for public release; further dissemination unlimited.



**Sandia National Laboratories**

Issued by Sandia National Laboratories, operated for the United States Department of Energy by Sandia Corporation.

**NOTICE:** This report was prepared as an account of work sponsored by an agency of the United States Government. Neither the United States Government, nor any agency thereof, nor any of their employees, nor any of their contractors, subcontractors, or their employees, make any warranty, express or implied, or assume any legal liability or responsibility for the accuracy, completeness, or usefulness of any information, apparatus, product, or process disclosed, or represent that its use would not infringe privately owned rights. Reference herein to any specific commercial product, process, or service by trade name, trademark, manufacturer, or otherwise, does not necessarily constitute or imply its endorsement, recommendation, or favoring by the United States Government, any agency thereof, or any of their contractors or subcontractors. The views and opinions expressed herein do not necessarily state or reflect those of the United States Government, any agency thereof, or any of their contractors.

Printed in the United States of America. This report has been reproduced directly from the best available copy.

Available to DOE and DOE contractors from

U.S. Department of Energy  
Office of Scientific and Technical Information  
P.O. Box 62  
Oak Ridge, TN 37831

Telephone: (865) 576-8401  
Facsimile: (865) 576-5728  
E-Mail: [reports@osti.gov](mailto:reports@osti.gov)  
Online ordering: <http://www.osti.gov/scitech>

Available to the public from

U.S. Department of Commerce  
National Technical Information Service  
5301 Shawnee Rd  
Alexandria, VA 22312

Telephone: (800) 553-6847  
Facsimile: (703) 605-6900  
E-Mail: [orders@ntis.gov](mailto:orders@ntis.gov)  
Online order: <http://www.ntis.gov/search>



SAND2016-0706  
Unlimited Release  
January 2016

# Metal-Organic Framework Thin Films as Stationary Phases in Microfabricated Gas-Chromatography Columns

Douglas Read\*

Dept. 2718, Active Ceramics Value Stream  
Dept. 1714, Bio/Chem/Physical Microsensors (at the time this work was performed)

Colin Sillerud

Dept. 1714, Bio/Chem/Physical Microsensors

\*Sandia National Laboratories

P.O. Box 5800

Albuquerque, New Mexico 87185-MS0963

## Abstract

The overarching goal of this project is to integrate Sandia's microfabricated gas-chromatography ( $\mu$ GC) columns with a stationary phase material that is capable of retaining high-volatility chemicals and permanent gases. The successful integration of such a material with  $\mu$ GCs would dramatically expand the repertoire of detectable compounds for Sandia's various microanalysis systems. One such promising class of candidate materials is metal-organic frameworks (MOFs). In this report we detail our methods for controlled deposition of HKUST-1 MOF stationary phases within  $\mu$ GC columns. We demonstrate: the chromatographic separation of natural gas; a method for determining MOF film thickness from chromatography alone; and the first-reported  $\mu$ GC  $\times$   $\mu$ GC separation of natural gas—in general—let alone for two disparate MOF stationary phases. In addition we determine the fundamental thermodynamic constant for mass sorption, the partition coefficient, for HKUST-1 and several light hydrocarbons and select toxic industrial chemicals.



## ACKNOWLEDGMENTS

This research is funded in whole by the Sandia National Laboratories, Laboratory Directed Research Development (LDRD) Program, Nanodevices and Microsystems Research Foundation (NMRF) Investment Area, through LDRD Project Number 173133, “Metal-Organic Framework Thin Films as Gas-Chromatography Stationary Phases for the Detection of Toxic Industrial Chemicals”.

A special thanks to: Dorina (Ina) Sava-Gallis (SNL Dept. 1124) for her expert guidance and help with MOF synthesis; Joe Simonson (SNL Dept. 1714) for being a *sound* sounding board for technical and programmatic advice; Bonnie McKenzie (SNL Dept. 1819) for her SEM imaging work; and Nathaniel Pfeifer (SNL Dept. 1714) for his work in writing the LabView program that operated the syringe pump apparatus.

# CONTENTS

1. Executive Summary .....	7
2. Introduction and Background .....	9
3. Experimental .....	11
3.1 $\mu$ GC Columns .....	11
3.2 MOF Deposition Methodology .....	13
3.3 Quartz-Crystal Microbalance .....	15
3.4 Gas Chromatography .....	15
3.5 Analyte Chemicals .....	16
4. Results & Discussion .....	17
4.1 Characterizing Deposition and Film Thickness Using QCM .....	17
4.2 HKUST-1 $\mu$ GC Separation of a Natural Gas Mixture .....	19
4.3 Characterizing HKUST-1 Sorption Thermodynamics for Controlling Chromatographic Performance .....	21
4.4 Determining the Relative Polarity of HKUST-1 .....	25
4.5 Determining MOF Film Thickness from Chromatography .....	26
4.6 Using Chromatography to Probe Layer-by-Layer Deposition Kinetics of SURMOF Thin Films on $\mu$ GC Column Channels .....	28
4.7 Determining Partition Coefficients for Toxic Industrial Chemicals and HKUST-1 Stationary Phases .....	32
4.8 Novel Comprehensive $\mu$ GC $\times$ $\mu$ GC Using MOF Stationary Phases for the 2D Separation of Natural Gas .....	33
5. Conclusions .....	39
6. References .....	40
7. Distribution .....	41

# 1. EXECUTIVE SUMMARY

The overarching goal of this project is to integrate Sandia's microfabricated gas-chromatography ( $\mu$ GC) columns with a stationary phase material that is capable of retaining high-volatility chemicals and permanent gases. The successful integration of such a material with  $\mu$ GCs would dramatically expand the repertoire of detectable compounds for Sandia's various microanalysis systems. One such promising class of candidate materials is metal-organic frameworks (MOFs). MOFs are crystalline materials containing inorganic clusters crosslinked by a rigid organic network. They are highly porous, thermally stable, and possess tunable chemical sorption affinity through modification of their chemical functionality and pore structure, making them well suited to small-molecule absorption. In this report, we demonstrate HKUST-1 and ZIF-8 MOF thin films as improved stationary phases for the high-speed, gas-chromatographic separation of high-volatility analytes and permanent gases. Layer-by-layer depositions are carried out in both fused silica capillary and  $\mu$ GC columns. A 1.2m $\times$ 630 $\mu$ m $\times$ 70 $\mu$ m  $\mu$ GC column coated with a 100nm HKUST-1 MOF film is able to completely separate the natural gas components methane through pentane within one minute, and with sufficient resolution to distinguish *iso*- from *n*-butane. Scanning Electron Microscopy is used to determine the mean HKUST-1 film thickness, which is correlated to the number of layer-by-layer deposition cycles. From thickness and chromatographic retention-factor measurements, we calculate a value for the partition coefficient of HKUST-1 as a function of temperature for seven analytes. HKUST-1 partition coefficients at 30°C are shown to be factors of 62 and 6.2 $\times$ 10<sup>3</sup> higher than those for a commercial polar PLOT phase, for *n*-butane and methanol, respectively. Determination of polar-to-non-polar analyte retention factor ratios provides a useful metric for quantifying the polar nature of HKUST-1—outperforming both of the polar polyethylene glycol and the U-Bond® PLOT phases in this regard. The layer-by-layer deposition of HKUST-1 films is monitored in situ using QCM, and morphology is subsequently determined with SEM. As a corollary, we are able to use measured retention-factors and now-known partition coefficients to calculate MOF film thicknesses deposited within  $\mu$ GC channels from chromatographic data alone. Subsequent comparison with SEM images detailing film morphology indicates a relatively high activation barrier, nucleation-driven, layer-by-layer deposition in which HKUST-1 islands form, and complete surface coverage does not occur until  $\sim$ 17 deposition cycles. Despite the chemical similarity, this nucleation phenomenon is not observed for SiO<sub>2</sub>-coated QCM depositions, which indicates that nuances of substrate surface chemistry and or preparation should be considered and that MOF deposition kinetics may not translate between seemingly similar substrates *a priori*.

The polar nature of HKUST-1 makes it an attractive stationary-phase candidate not only for natural gas but perhaps more appropriately for polar small-molecule analytes. One such class of analytes of great interest is that of highly volatile, Toxic Industrial Chemicals (TICs). TICs represent a large class of ubiquitous chemicals, which pose a threat to the environment and human life, though accidental or terrorist release. Traditional polymer stationary phases simply do not retain TICs effectively. Partition coefficients at 50°C are measured for the select TICs: chlorine gas, chloromethane, carbon disulfide, and methylene chloride as proof-of-concept data for using MOF stationary phases for the retention of these challenging analytes. These analytes are indeed retained by HKUST-1 with partition coefficients ranging between those of ethane and propane. Additionally we report the first comprehensive  $\mu$ GC $\times$  $\mu$ GC separation of light

hydrocarbons—in general—let alone with using disparate MOFs (HKUST-1 × ZIF-8) as the stationary phases.

## 2. INTRODUCTION AND BACKGROUND

A great deal of effort has been put forth in recent years for the development and optimization of portable chemical detectors. At the heart of portable chemical detection criteria is that the unit must have lowpower consumption, be compact and lightweight, and have a high degree of discrimination power (selectivity for broad range of analytes against interferents). Additional criteria include: fast analysis times (< 1 min. for early warning applications); extremely high reliability and low false-alarm rates. One such scheme to address portable detection is the *lab-on-a-chip* platform which uses microfabricated gas chromatography  $\mu$ GC columns.<sup>[1]</sup>  $\mu$ GC columns address several of the most vexing problems for a portable system, such as: increased chromatographic efficiency for high speed; increased resolution (peak capacity); and fast, low-power temperature programming. The high aspect ratio of  $\mu$ GC channel dimensions is of advantage for increasing chromatographic efficiency (higher number of theoretical plates) for given column length and flow impedance. As compared with typical capillary GC columns,  $\mu$ GC columns have low thermal mass and therefore require much less power to temperature program and heat up and they especially cool down more quickly, thereby minimizing the analysis-cycle time. MEMS heaters and RTD temperature sensors can be integrated on-chip with the  $\mu$ GC for additional power and time savings.

$\mu$ GC research, at Sandia and elsewhere, has typically been focused on the detection of volatile organic chemicals (VOCs) and semi-VOCs such as chemical warfare agents (CWAs). Stationary phases for  $\mu$ GC columns are typically polymers. Polymer phases are well understood, straight forward to coat, and the phase ratio (polymer film thickness) can easily be controlled for tuning chromatographic performance. Simply put, polymers work well for retention of VOCs and semi-VOCs. However, polymer stationary phases simply don't have the necessary retention power for the separation of high-volatility analytes (i.e. volatilities >  $n$ -C<sub>8</sub>H<sub>18</sub>). As such, current Sandia  $\mu$ GC columns in their current configuration are not suited to the detection of this class of chemicals because of these analytes' poor retention characteristics on traditional polymer sorbent materials. A need exists for a material that can fill this gap in chem-detection capabilities. In addition, high-polarity polymers such as PEG suffer from degradation in air (especially at elevated temperatures) and air is often the carrier gas of necessity for portable systems for the simplification of not having consumable high-pressure gas cylinders. There is ever-increasing interest in detecting light analytes with a field-deployable system. Many of these light chemicals of interest fall under the classification of toxic industrial chemicals (TICs), which are often polar and typically have high volatility or are permanent gases. Examples of TICs include: ammonia, chlorine, hydrogen sulfide, sulfur dioxide, hydrogen cyanide, and formaldehyde. Industry applications include: natural gas field analysis, chemical manufacturing and transport safety, first responder hazard warning and identification, and homeland defense and military (terrorist release or illegal military use). The illegal use of chlorine gas as a warfare agent is one such pertinent example.

Very little has been reported on the use of  $\mu$ GC columns for detection of high-volatility and permanent-gas analytes. One such article is that of Lefebvre et al.<sup>[2]</sup> wherein they demonstrate the separation of light alkanes using a  $\mu$ GC column coated with a sol-gel stationary phase. This is encouraging, but control of thickness and therefore chromatographic tuning has yet to be demonstrated.

Other stationary phases suited to high-volatility chem detection in traditional, non-portable GC include Porous Layer Open Tubular (PLOT) and packed-particle phases. Packed particle

columns suffer from chromatographic band/peak broadening (especially for high-speed GC) and therefore do not have sufficient peak capacity (peak resolution). In addition,  $\mu$ GC columns are hard to pack with particles, and the large thermal mass is antithetical to efficient heat transport for fast, low-power thermal cycling. PLOT phases offer an advantage over traditional polymers, however their formulation is proprietary and thus inaccessible for in-house coating of non-commercial  $\mu$ GC columns. New stationary-phase materials are needed for this application. MOFs represent a class of materials that can be tuned in terms of their chemical functionality and pore size and as such make an attractive class for stationary phases.

Metal-organic framework (MOF) materials have been extensively studied for their extreme gas absorption properties and as such are a promising candidate for high-speed, small-molecule GC separation. MOFs are crystalline materials that consist of organic ligand *struts* that bridge inorganic centers (typically metals or metal clusters). The MOF structure is templated by the specific ligand used in the synthesis. MOFs are highly porous, thermally stable, and possess tunable chemical sorption affinity/selectivity through modification of their chemical functionality and pore structure. Certain MOFs can also be deposited using layer-by-layer techniques directly on select substrates as conformal thin films.<sup>[3,4]</sup> These so called surface-mounted MOFs (SURMOFs) allow for the direct deposition of a MOF thin film with a known thickness, both attributes being ideal from a chromatography perspective.

Gu et al. and Xie et al.<sup>[5,6]</sup> have reported on the deposition of MOF crystals adhered to the walls of fused silica capillary for the separation of xylene isomers and chiral compounds, respectively. Here we detail experiments with the layer-by-layer deposition of surface-mounted, conformal MOF thin films in both microfabricated silicon GC columns and commercial fused silica capillary. Stavila et al. as well as Wöll, and Fischer et al. have all detailed the methods and rates of LBL HKUST-1 film growth on various substrates.<sup>[7-9]</sup> Here we are concerned with the application of these thin films as stationary phases for GC, particularly high-speed  $\mu$ GC.

### 3. EXPERIMENTAL

#### 3.1 $\mu$ GC Columns

In this research we use three types of  $\mu$ GC columns fabricated with dimensions as follows:

nominal dimensions	channel	column name/label		
		70-120	30-90	30-30
depth ( $\mu\text{m}$ ):		685	685	685
width ( $\mu\text{m}$ ):		70	30	30
length (cm):		120	90	30

These high-aspect-ratio  $\mu$ GC columns are fabricated by a Bosch-process, Deep Reactive-Ion Etch (DRIE) of  $\langle 1\ 0\ 0 \rangle$  Si. A  $\sim 1\mu\text{m}$  thermal oxide is grown on the channel walls leaving a nominally hydroxylated  $\text{SiO}_2$  surface. Capillary ports are left sealed with a thin membrane of silicon to prevent silicon debris particles from entering and packing the column during the dicing stage.<sup>[10]</sup> This membrane seal is easily punctured with a metal pin and breakage debris is minimal and can be sucked out with vacuum leaving a pristine oxide channel. Previous Sandia  $\mu$ GC versions did not have this hermetic seal and water-borne saw debris from the dicing process would create a packed bed of silicon microparticles that could not be removed (figure 1 c&d). 5cm of 630 $\mu\text{m}$ OD x 200 $\mu\text{m}$ ID polyimide coated, fused silica capillary (Molex Inc. Polymicro-Technologies<sup>TM</sup> special order) are epoxied (Henkel Inc. Loctite<sup>®</sup> 1CTM Hysol<sup>®</sup> two part epoxy) at 80 $^\circ\text{C}$  into both the inlet and outlet ports on the  $\mu$ GC for connection to either a commercial gas chromatograph or the SURMOF deposition apparatus. Pictures and SEM micrographs of the  $\mu$ GC chip are shown below in figure 1.

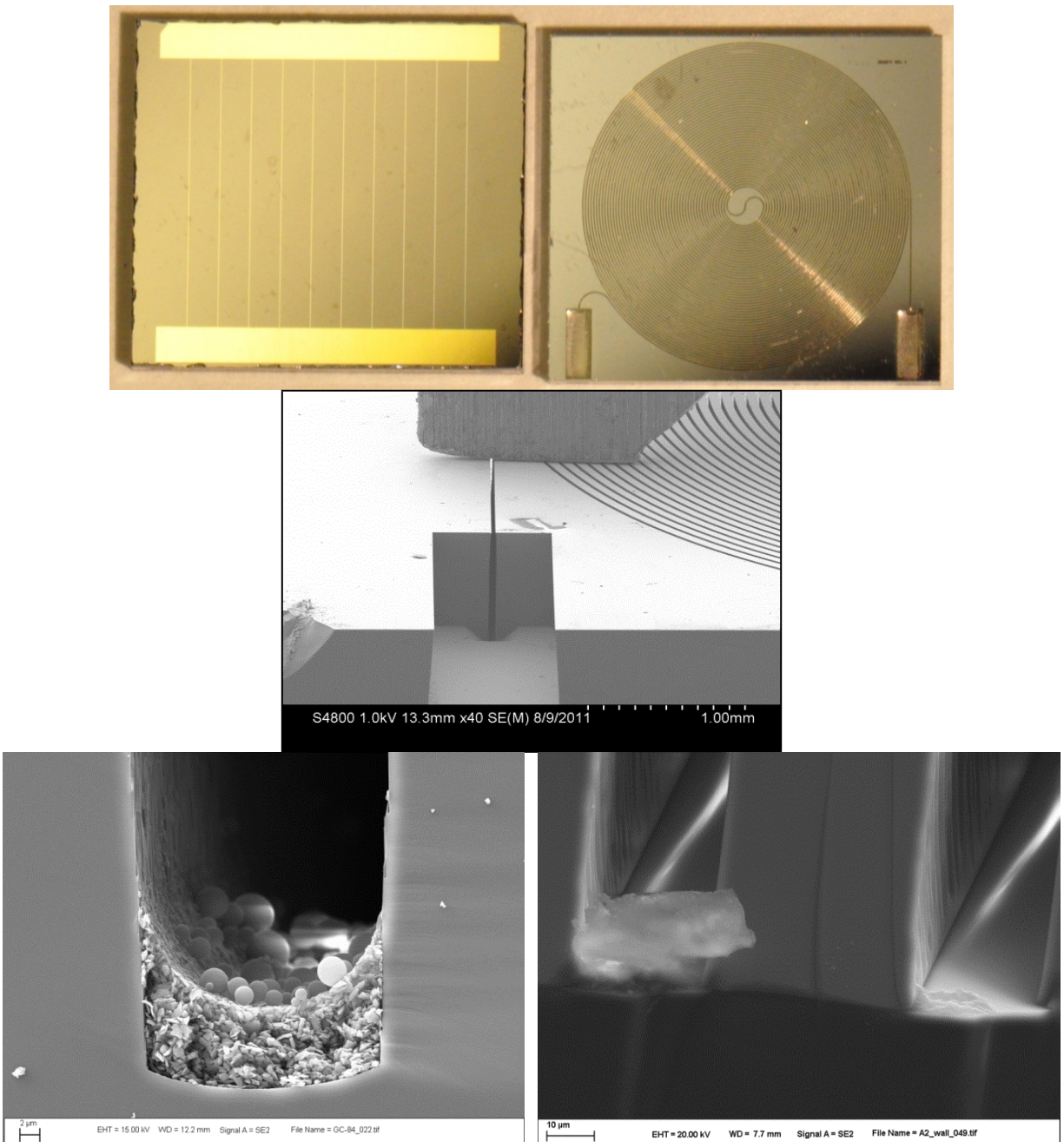


**Figure 1.** (a) Pictures of the top and bottom of latest-model Sandia microfabricated GC ( $\mu$ GC) column with nominal channel dimension of  $70 \times 685 \mu\text{m} \times 120 \text{cm}$  Bosch etched in silicon and capped with an anodically bonded glass lid. The dimensions of the  $\mu$ GC column are  $\sim 1 \times 1 \text{cm}$ . A MEMS heater is integrated into bottom of the chip of efficient and fast temperature programming. Capillary ports are left sealed with a thin membrane of silicon during dicing to prevent saw debris from entering the channel. (b) An SEM micrograph of a  $30 \times 685 \mu\text{m} \times 90 \text{cm}$   $\mu$ GC column illustrates the extremely high aspect ratio of the channels. (c) Dicing saw debris trapped in a  $\mu$ GC column that did not have protective Si membrane seal during dicing. (d) An SEM micrograph of similar channels as (c), but with the use of the Si membrane seal during dicing illustrates the utility of the method for keeping the channels free of debris.

## 3.2 MOF Deposition Methodology

The conformal HKUST-1 (Hong Kong University of Science and Technology-1) thin films were deposited using the layer-by-layer method developed by Wöll and Fischer et al.<sup>[7,8]</sup> and subsequently reproduced and kinetically characterized on various substrates by Stavila et al.<sup>[9]</sup> Here we modify the deposition pumping equipment from peristaltic pumps<sup>[9]</sup> to enable the high pressures necessary to push the HKUST-1 reactant solutions through the  $\mu$ GC channel. This was accomplished by using syringe pumps (Harvard Apparatus models PHD2000 and 33) controlled by a LabView® program to alternate between a flow of 0.2mM copper(II) acetate,  $\text{Cu}(\text{OAc})_2$ , in ethanol and 1.0mM trimesic acid ( $\text{H}_3\text{btc}$ ) in ethanol (each reactant cycle is followed by a pure ethanol rinse cycle to prevent the reactants from reacting in solution). Ethanolic solutions were prepared before every deposition. The temperature of the reaction is kept at a constant 50°C. Reagent chemicals are purchased from Sigma Aldrich and are all reagent grade.

Reaction of the reagents in solution is unwanted so the flow-system is designed such that the solutions do not come into direct contact with one another at any point during the deposition. We have found it necessary to place a solenoid valve (NRResearch Inc., Teflon wetted part #: HP161T032) in line after each syringe pump to ensure that flow is completely stopped when the syringe pump is not operating due to the continuation of flow resulting from built up pressure in the syringes. Additionally, PEEK tubing and fittings (Valco Instruments Co. Inc.) are used to prevent unwanted SURMOF growth on the supply tubing. The flowrate of each sub-cycle ( $\text{CuOAc}/\text{EtOH}$ , trimesic acid  $\text{EtOH}$ , and  $\text{EtOH}$  rinse) was set such that five times the volume of the micro column and supply tubing are pumped for each sub cycle during a 10 min period. Temperature is controlled with either a hotplate or a laboratory oven and is measured with a thermocouple and recorded throughout the deposition. This volume and time normalized flowrate allows for equivalent deposition despite changing flow cell/column volumes (such as a QCM flow cell). For the  $\mu$ GC columns used in this research, the flowrates are set to 150 $\mu\text{L}/\text{min}$ . A schematic and picture of the flow apparatus are shown in [figure 2](#) below. Energy Dispersive X-ray Spectroscopy (EDS) is employed to verify the chemical composition of the deposited MOF films (EDS micrographs are presented in [figure 3](#) below).

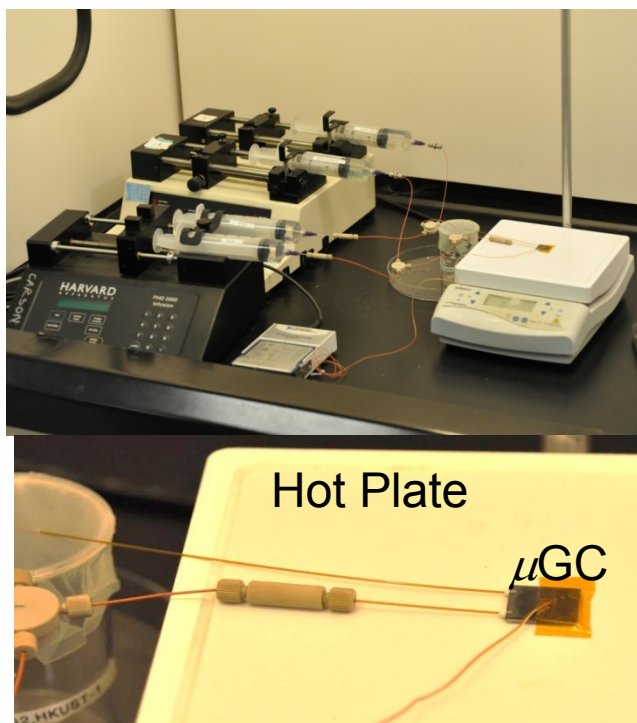
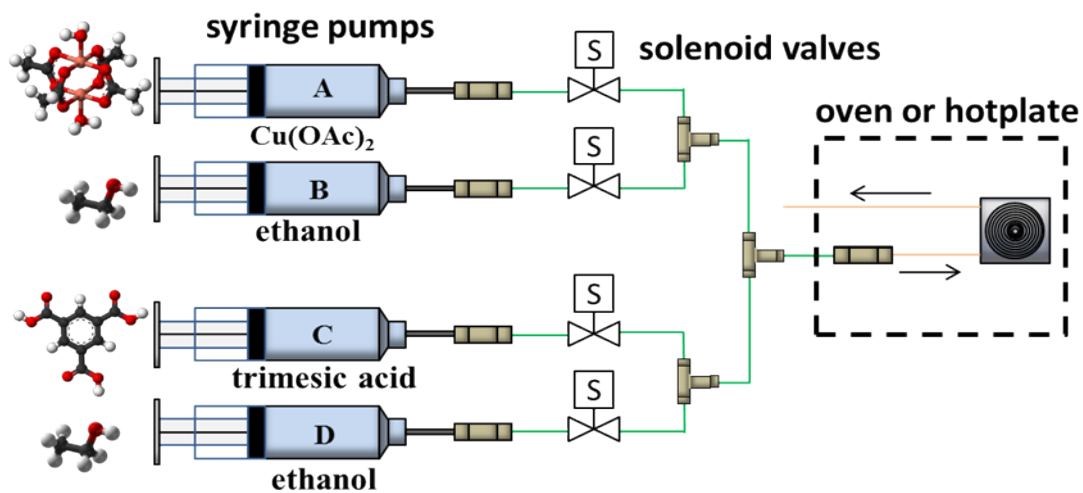


**Figure 2.** (a) Schematic detailing the syringe-pump, layer-by-layer deposition apparatus. (b) Pictures of the actual MOF deposition apparatus and  $\mu$ GC column.

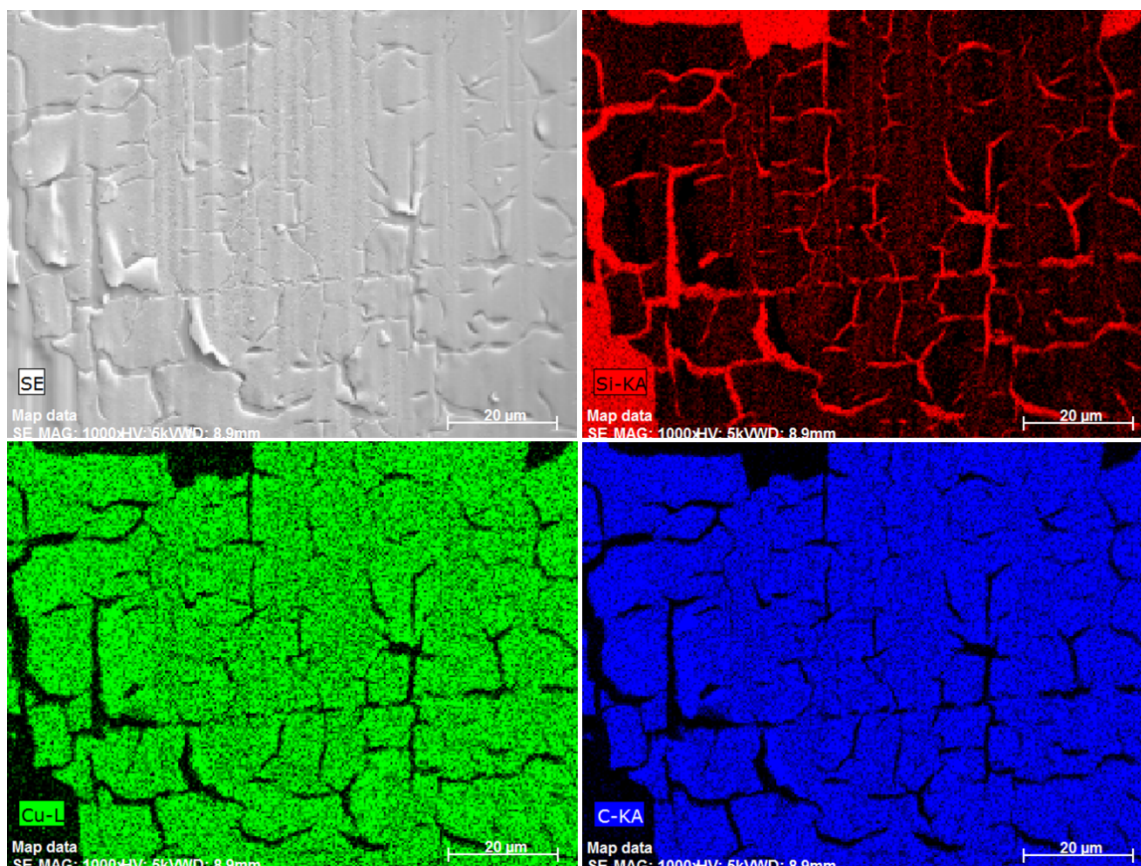


**Figure 3.** Energy Dispersive X-ray Spectrographs (EDS) illustrate the high levels of silicon within the cracks in the film and the high levels of copper and carbon within the film itself. (The top left micrograph is a standard SEM image).

### 3.3 Quartz-Crystal Microbalance

The quartz-crystal microbalance (QCM) system used in this research is the Maxtek (now Inficon) RQCM PLO-10i phase lock oscillator with OEM crystal holder/flow cell. The 5MHz resonant frequency quartz crystals are 25.4mm in diameter and are coated with an outer layer of SiO<sub>2</sub> to best match the surface of the  $\mu$ GC channels (Inficon part #: 149277-1). The temperature of the reaction was maintained at a constant 50°C by a laboratory oven (temperature was also monitored and recorded throughout the deposition). Crystals were cleaned immediately prior to the deposition by UV-ozonation for 30min. Frequency measurements were recorded *in situ* and dry, room-temperature frequency measurements were recorded before and after MOF depositions.

### 3.4 Gas Chromatography

Hydrocarbon and methanol chromatography was performed on an Agilent 7890N GC with an auto injector and flame ionization detector (FID). A 1 mm ID Siltek®-Deactivated Uniliner® inlet liner (offered by Restek Corp. part #: 21053-214.5) was used with split-inlet flow (split ratios vary).  $\mu$ GC-column flow connections were made from the GC inlet and to the FID using 250 $\mu$ m ID deactivated fused silica Rxi® Guard capillary pigtailed at 30 and 22cm,

respectively (Restek Corp. part 10029). Interconnect union fittings used for this arrangement are CapTite™ unions made of Ultem® (available from LabSmith, Inc.). Comprehensive, stop-flow  $\mu$ GC $\times$  $\mu$ GC chromatograms were generated using the Agilent 7890N as described above, but with the second pressure-controlled GC inlet connected to a miniaturized 24VDC solenoid *spider* valve for modulating flow between the two columns (Staiger GmbH & Co. part # 604 000 269, distributed by Humphrey Inc. part # VA 204-716 E 07 SAL 80 24/00). The valve seat used for gas connections is custom designed (Sandia Labs and GenTech Concepts LLC) and machined (TEAM Technologies Inc.). Valve modulation is accomplished with a LabView program and GC $\times$ GC chromatograms are generated using an in-house written MATLAB program. Chlorine retention data was measured with a LECO Corp. Pegasus® 4D GC $\times$ GC time-of-flight mass spectrometer in 1-D chromatography mode using the same configuration as that of the 7890N except for a longer 50cm pigtail from the  $\mu$ GC to the detector.

### 3.5 Analyte Chemicals

Natural gas samples are Scotty® 14 natural gas standard (Scott Specialty Gases, now Air Liquide) in the following composition (mol%): balance methane; 12.5 % ethane; 3.02% *n*-butane 3.05% *i*-butane; 0.503% *i*-pentane; 6.96% propane; with other trace gases CO<sub>2</sub> and N<sub>2</sub>. Where noted, additional pure propane, butane mixtures, and liquid-headspace *n*-pentane and/or *n*-hexane were added to the GC vial with the Scotty gas to increase the relative analyte proportions. Chlorine gas was generated by reacting concentrated hydrochloric acid with trichloroisocyanuric acid (CAS: 87-90-1, E-Z CLOR® pool water sanitizer). Warning: chlorine gas is a strong oxidizer that is highly toxic. Great care should be observed to avoid inhalation and exposure in general (i.e. use of fume hood and personal protective equipment by trained and knowledgeable personnel).

## 4. RESULTS & DISCUSSION

### 4.1 Characterizing Deposition and Film Thickness Using QCM

The *in situ* monitoring of the progress of the MOF deposition and the determination of film thickness is performed using a quartz-crystal microbalance (QCM) with a 5MHz, polished SiO<sub>2</sub>-coated crystal. After the final ethanol rinse for each cycle, all syringe pumps are stopped and solenoid valves are closed. This allows for a perfectly quiescent stage where a consistent frequency measurement is recorded between every deposition cycle. For thickness calculations, the Sauerbrey equation and an HKUST-1 specific gravity of 0.76 is used as reported by Stavila et al. for their similarly deposited thin films.<sup>[9]</sup> The *in situ* QCM frequency data are presented in [figure 4a&b](#) for a 40-cycle layer-by-layer deposition of HKUST-1. These data yield a final HKUST-1 film thickness of 264nm with an average single deposition-layer thickness of 6.6 nm. [Figure 4c](#) shows the individual thickness measurements as a function of deposition cycle. These values are higher than those reported by Stavila et al. and higher than the 168nm calculated by measuring the crystal's frequency in air at 23°C before and after the deposition. The oscillator was *capacitance matched* dry at 23°C (where the first frequency measurement was taken); then matched in ethanol at 50°C (for the *in situ* measurement; and then dried in a stream of nitrogen, cooled to 23°C, capacitance matched (this is the post-deposition dry measurement). The reason for these discrepancies is not known, but it is likely that absorbed EtOH during the deposition could account for this discrepancy. Also of note is that the deposition rate (change in film thickness) decreases with increasing deposition-cycle number. One observation that could explain the decrease in layer thickness is that the H<sub>3</sub>btc does not seem to fully react within the 10min sub-cycle as the deposition progresses (i.e. the reaction rate of H<sub>3</sub>btc step is slowing down as the film grows). It is hypothesized that this is due to a mass transport limitation as the surface area of the MOF film increases. Regardless of the reason, it is recommended for future experiments that the time allotted for each deposition cycle should be increased until there is evidence that the reaction is complete.

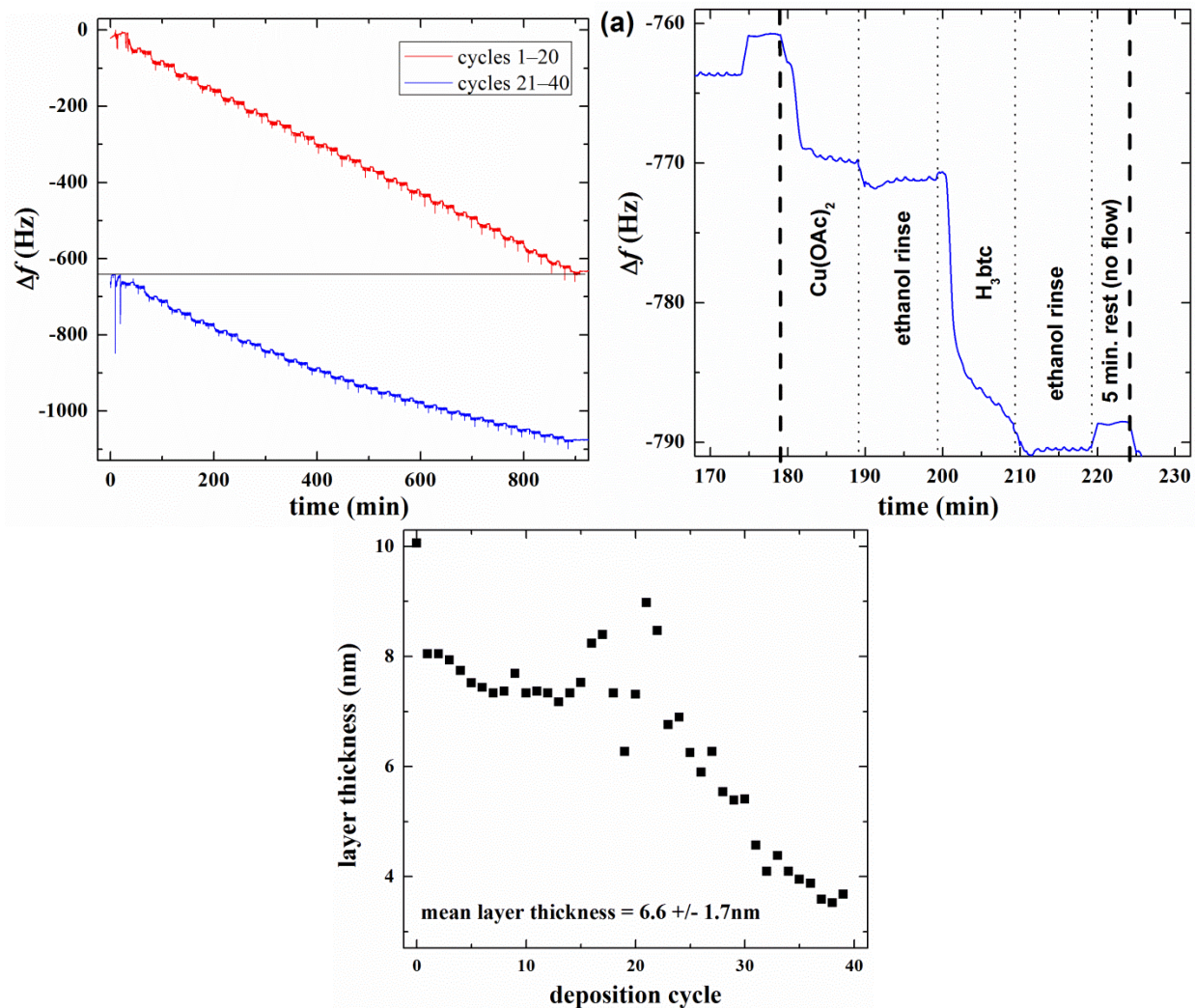


**Figure 4.** (a) *In situ* QCM frequency data for a 40-cycle deposition of HKUST-1 on  $\text{SiO}_2$ -coated quartz crystal. The data are split into two plots because it was necessary to run two back-to-back depositions of 20 cycles because of limited syringe volume. (b) This plot is a detailed view of the QCM frequency change for one complete deposition cycle. Note that that for this cycle at  $\sim 200$ min on the 21–40 cycle plot, the QCM does not reach an equilibrium frequency for the  $\text{H}_3\text{btc}$  step. (c) Plotting the deposited layer thickness shows a decrease in the deposition rate with increasing deposition-cycle number. This may be due to the increasingly slower reaction of  $\text{H}_3\text{btc}$  as the deposition progressed as seen in (b) above.

## 4.2 HKUST-1 $\mu$ GC Separation of a Natural Gas Mixture

A  $\mu$ GC column (630 $\mu$ m x 70 $\mu$ m x 120cm with 10cm total 250 $\mu$ mID capillary) was coated with a 35-layer HKUST-1 film (~65nm) at 50°C. A chromatogram was taken with an Agilent 7890 benchtop GC with an FID detector. We employed a temperature ramp from 22 to 150°C at an oven ramp rate of 30°C/min (indicated by the instrument but not measured for the  $\mu$ GC column itself) with a hydrogen carrier gas at 15psi hydrogen (flowrate and velocity). A small amount of neat *n*-pentane and *n*-hexane were added to the bottom of the GC vial (for a total liquid depth of 2mm) and the vial was then filled with a natural gas mixture (Supelco SCOTTY 14, see experimental section for details). The chromatogram shown in [figure 5a](#) below illustrates the exceptional ability of these HKUST-1 films in separating light hydrocarbon mixtures. Here we see the separation of C1–C5 in one minute with sufficient resolution to discriminate between *iso*- and *n*-butane. Alternatively, an identical  $\mu$ GC column was coated with a surface-bonded 300nm thin film of OV-1 (Ohio-Valley Inc. polydimethylsiloxane, or PDMS). Unlike the HKUST-1 phase, the PDMS phase is unable to retain and separate this same light hydrocarbon mix. This is evidenced by the single peak shown in the chromatogram in [figure 5b](#) below.

Recently Lefebvre<sup>1</sup> et al. have demonstrated the first  $\mu$ GC separation of natural gas using a sol-gel stationary phase.<sup>[2]</sup> Here we offer an alternative stationary phase that can be tuned in terms of its chemical functionality and pore size and the thickness of the film (and therefore the retention factor) can be carefully controlled—as we will demonstrate.

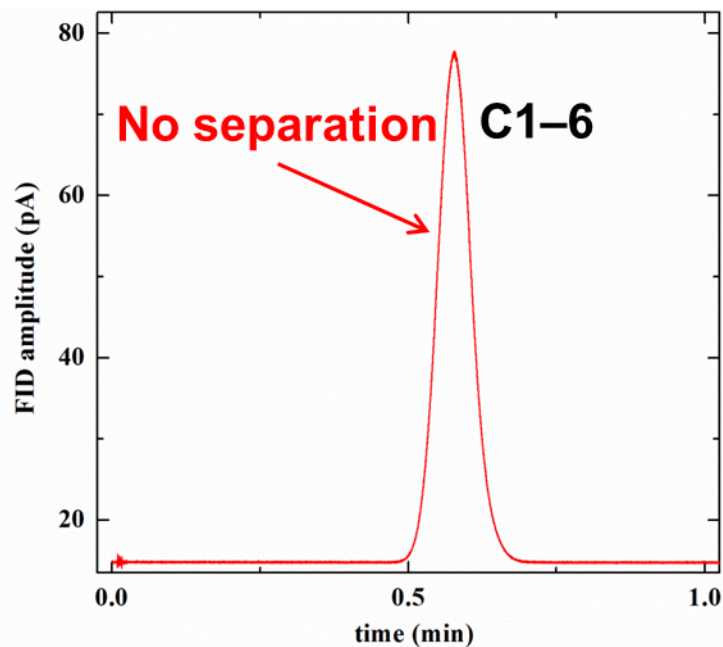
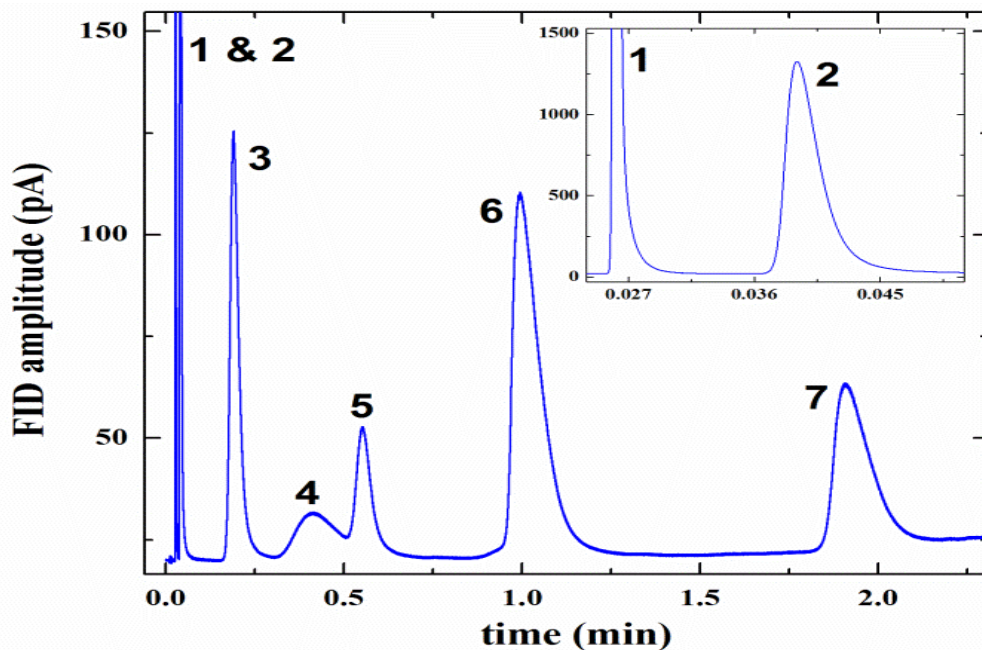


**Figure 5. (a)** The chromatogram for a 35-layer HKUST-1 coated 70-120  $\mu$ GC column showing the complete separation of natural gas (C1 – C6) with separation of C1–C5 within  $\sim$ 1 min. Note that there is sufficient chromatographic resolution for the separation of methane from ethane and the isomers *n*- and *i*-butane. Analytes: <sup>(1)</sup> Methane, <sup>(2)</sup> ethane, <sup>(3)</sup> propane, <sup>(4)</sup> *i*-butane, <sup>(5)</sup> *n*-butane, <sup>(6)</sup> *n*-pentane, <sup>(7)</sup> *n*-hexane. T ramp: 22–150°C at 30°C/min H<sub>2</sub> carrier gas at 15psig inlet pressure. **(b)** The chromatogram for 70-120  $\mu$ GC column coated with a traditional polymer stationary phase (bonded, 300nm PDMS) shows that there is no separation for the natural gas mixture.

### 4.3 Characterizing HKUST-1 Sorption Thermodynamics for Controlling Chromatographic Performance

We are primarily interested in developing a stationary phase that is highly retentive and polar and therefore has large retention factors for light polar analytes such as TICs. The fundamental metric for retention power of a particular stationary phase for a particular analyte is the partition coefficient,  $K$ . The partition coefficient is a temperature-dependent, intensive property of the stationary-phase/analyte pair and is therefore independent of the stationary-phase thickness. In essence, the partition coefficient is a measure of the amount of analyte a stationary phase can absorb at a particular concentration of analyte vapor. Figure 6 qualitatively illustrates the sorption process and the partition coefficient. The partition coefficient is related to the chromatographic retention time of an analyte through the following equations:

$$k(T) = K_{i,j} / \beta = \frac{t_{R,i} - t_M}{t_M} \quad \dots \text{Eq. 1}$$

$$\beta_j \equiv \frac{V_{col}}{V_j} = \frac{h \cdot w}{2 \cdot d_{f,j} (w + h - 2 \cdot d_{f,j})} \quad \dots \text{Eq. 2}$$

Here  $k$  is the retention factor, which is a measure of the retention time,  $t_R$  for the analyte,  $i$ , relative to the retention time of an unretained analyte (such as methane),  $t_M$ .  $\beta$  is the phase ratio and is defined as the ratio of free volume of the column to the volume of the stationary phase, and, in this case, written for a column with rectangular channels as in a  $\mu$ GC column. Here,  $h$  and  $w$  are the channel height and width and  $d_f$  is the film-thickness of the particular stationary phase  $j$ . (We will use the notation  $i$  and  $j$  throughout this report to represent the *analyte* and *stationary phase*, respectively.) The mean MOF film thickness and exact column dimensions were obtained by scanning electron microscopy using five measurements for each of three disparate number-of-cycle  $\mu$ GC columns which had been previously chromatographically characterized (i.e.,  $k(T)$  was determined for several analytes).

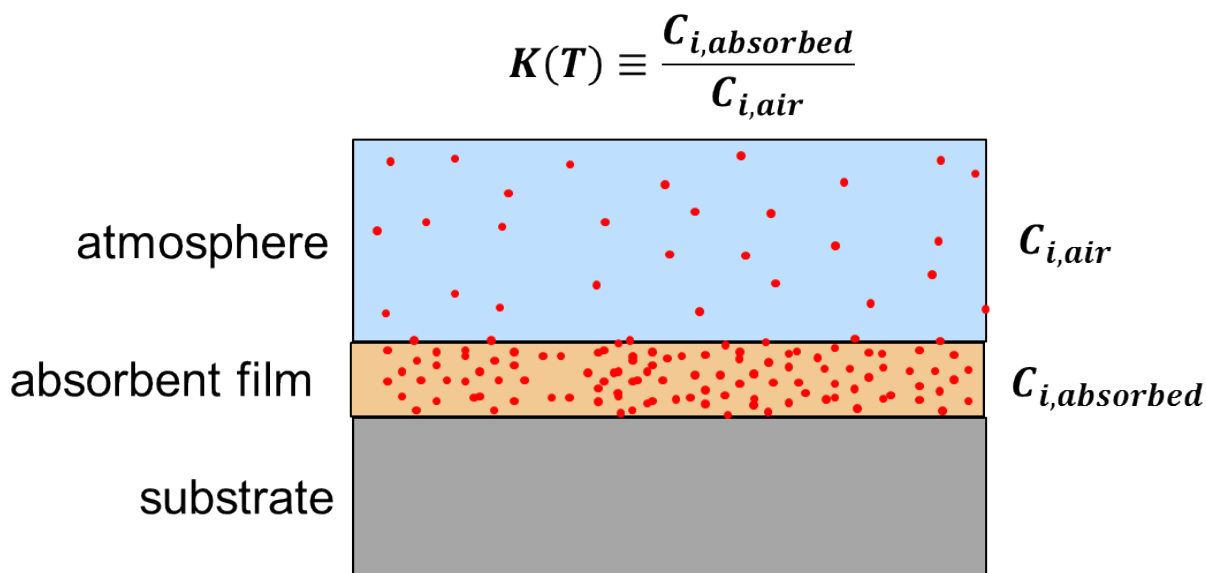


**Figure 6.** This schematic representation of equilibrium analyte absorption serves to qualitatively explain the thermodynamic sorption constant,  $K$ . Here we see that  $K$  at certain temperature is defined by the concentration of absorbed analyte in the stationary phase divided by the concentration of analyte in the environment to which the phase is exposed.

The partition coefficient is calculated from the stationary phase thickness and the column dimensions as measured using scanning electron microscopy (SEM) (see [figure 6 a & b](#) below), and from retention factor,  $k$ , which is chromatographically determined as a function of temperature. These data are represented by the so-called Van't Hoff equation (and plot), which is of the form:

$$\ln(K) = \ln(k \cdot \beta) = A + \frac{B}{T}, \quad \dots \text{Eq. 3}$$

It is noteworthy that the intercept,  $A$ , multiplied by the ideal gas constant,  $R$ , is the entropy of solution (i.e. sorption) for the analyte and stationary phase, or  $\Delta S_{soln,ij}$ . The slope,  $B$ , multiplied by  $R$  is the enthalpy of solution,  $\Delta H_{soln,ij}$ .

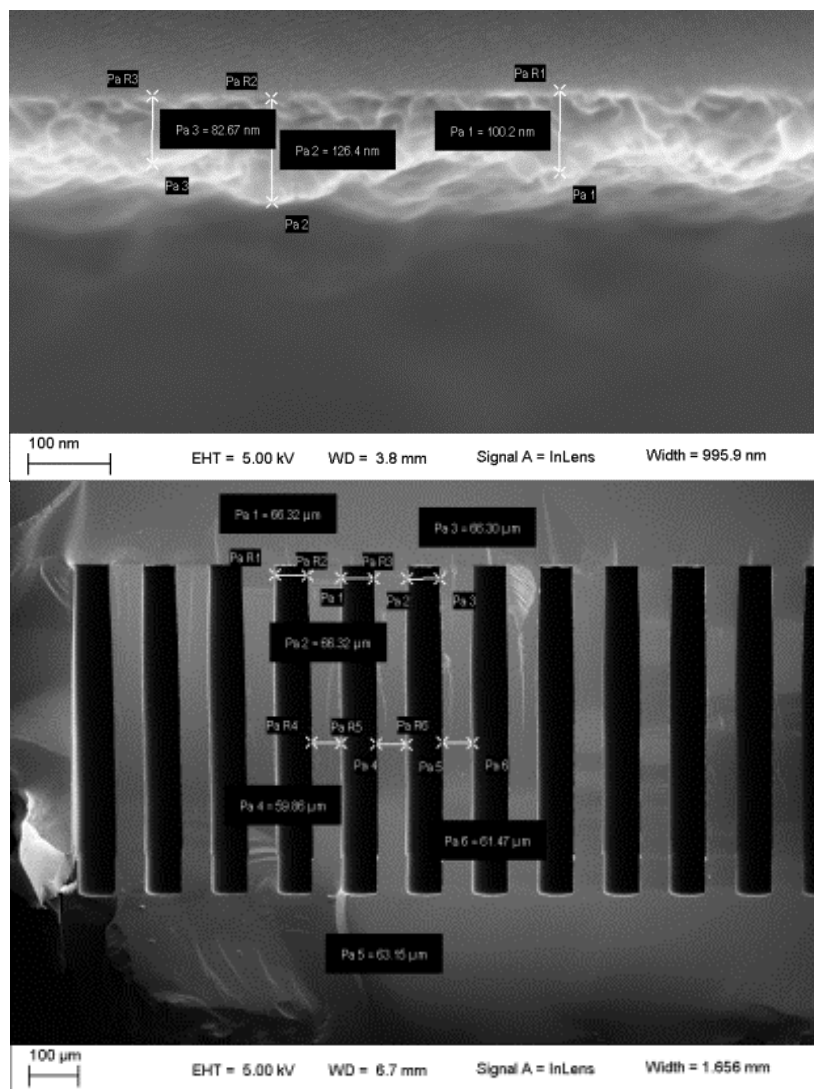


**Figure 6. (a)** SEM micrograph used to determine the mean HKUST-1 film thickness for coated  $\mu$ GC columns with particular numbers of deposition cycles (in this case 60 cycles). **(b)** SEM was additionally used to independently measure the actual  $\mu$ GC column channel dimensions. Both measurements were used to calculate the partition coefficients for HKUST-1 and select analytes.

**Figure 7** contains Van't Hoff plots for the HKUST-1 and the commercial, Rt-U-Bond® PLOT (Restek Inc.) stationary phases for various polar and non-polar, high-volatility analytes. The HKUST-1 column is a  $70 \times 685 \mu\text{m} \times 120 \text{cm}$   $\mu$ GC column with 35 deposition cycles ( $d_f = 65 \text{nm}$  and  $\beta = 464$  determined chromatographically, see following section). The Restek Rt-U-Bond is a capillary column specifically designed for retention of high-volatility *polar* compounds and has a diameter of  $320 \mu\text{m}$  and is cut to  $120 \text{cm}$  with  $d_f = 10 \mu\text{m}$  ( $\beta = 8$ ). Here we see that HKUST-1 consistently outperforms the PLOT column for the non-polar hydrocarbons and vastly outperforms it for the polar TIC surrogate methanol. Quantitatively, for methanol the HKUST-1 column has a partition coefficient of 1214 at  $150^\circ\text{C}$ , whereas the value for the U-Bond column is 3.6—this is an increase of 33,900%. The parameters for the linear fit of these data in **figure 7** to the Van't Hoff equation are given in **Table I**, below.

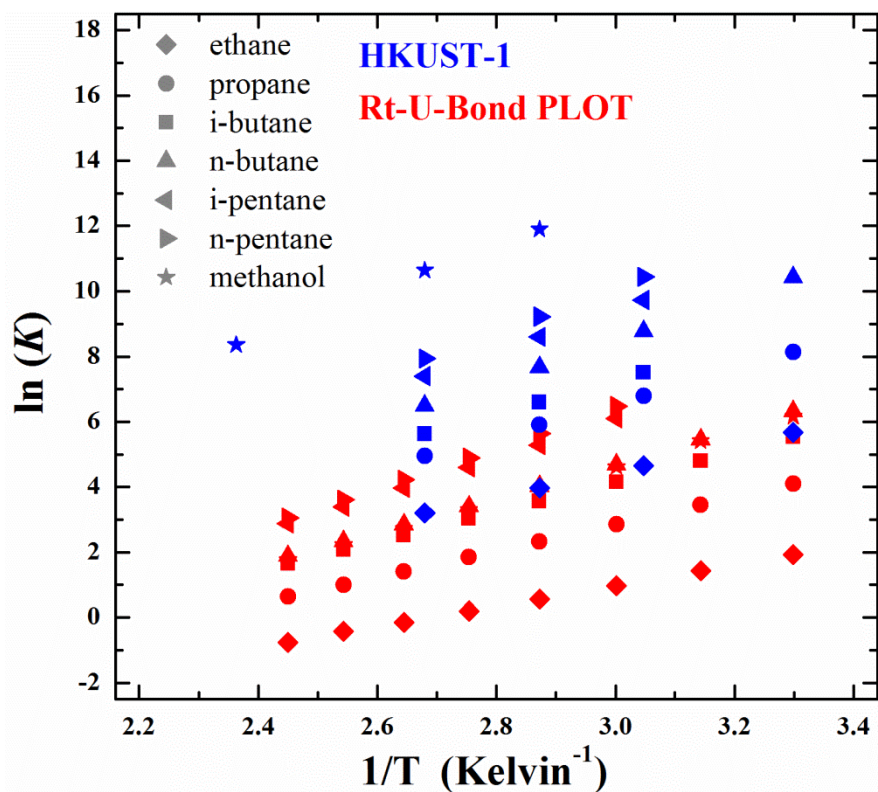


**Figure 7.** Van't Hoff plots for several analytes with both HKUST-1 and the commercial Rt-U-Bond PLOT phases illustrates a marked improvement of HKUST-1 over the PLOT phase especially for the polar TIC surrogate, methanol. Quantitatively HKUST-1 has a 33,900% higher partition coefficient than U-Bond at 150°C.

**Table I.** Constants and Pearson coefficients for the Van't Hoff data in figure 7.

	ethane	propane	<i>i</i> -butane	<i>n</i> -butane	<i>i</i> -pentane	<i>n</i> -pentane	methanol
<b>HKUST-1</b>	<b>A</b>	3974	5166	5112	6365	6351	6979
	<b>B</b>	-7.451	-8.919	-8.078	-10.592	-9.628	-10.387
	<b>R<sup>2</sup></b>	1.000	1.000	1.000	1.000	1.000	0.999
<b>U-Bond</b>	<b>A</b>	3137	4079	4577	5219	5834	6202
	<b>B</b>	-8.435	-9.371	-9.577	-10.943	-11.449	-12.163
	<b>R<sup>2</sup></b>	1.000	1.000	1.000	1.000	0.999	1.000

Van't Hoff equation:  $\ln(K) = A + B/T(\text{Kelvin})$

#### 4.4 Determining the Relative Polarity of HKUST-1

Since we are interested in the relative magnitude of the polarity of HKUST-1 for use as a stationary phase it is useful to develop a quantified metric for comparison to other candidate materials. One such method is calculating the retention time ratio of a polar to a non-polar analyte for each stationary phase at the same isothermal chromatographic conditions. In this case we use the retention time ratio of methanol to propane. The bar graph comparing HKUST-1 to U-Bond PLOT and polyethylene glycol (PEG) polymer columns is given in figure 8 below. Methanol-to-propane retention time ratios are 89, 7, and 2 for HKUST-1, U-Bond, and PEG, respectively. This translates to 12- and 45-fold increases in the relative polarity of HKUST-1 over U-Bond and PEG by this metric.

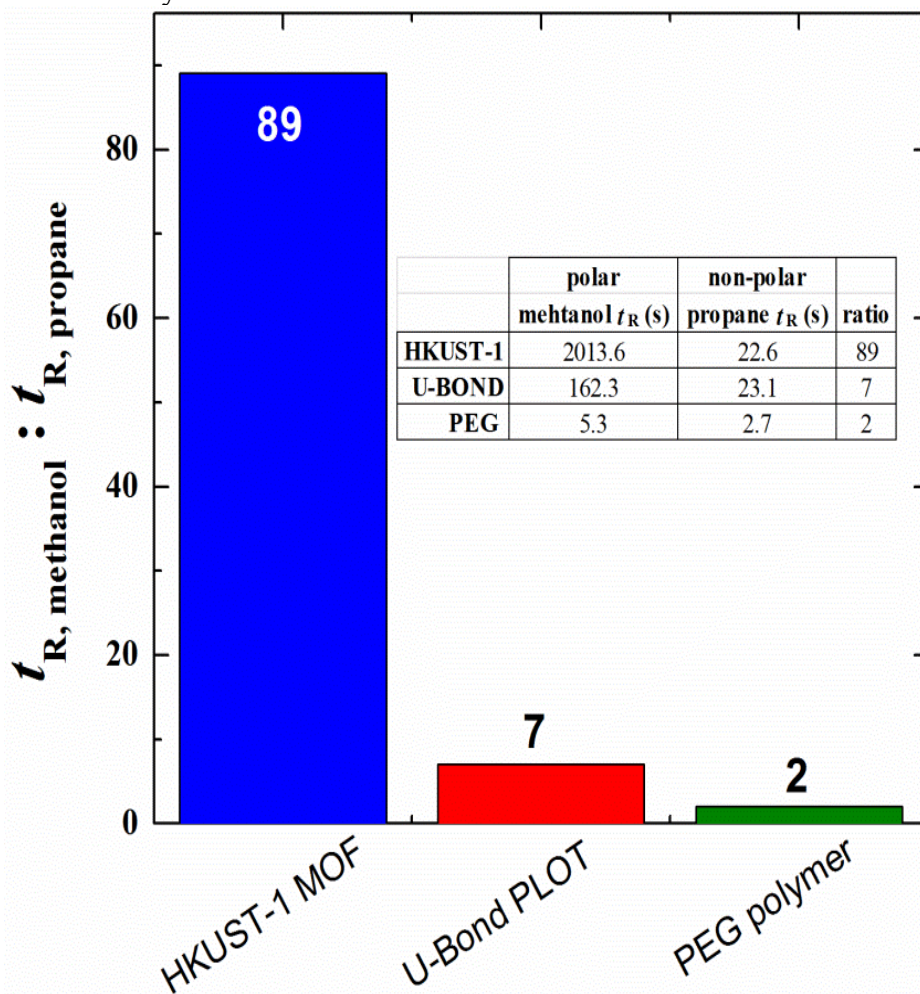


**Figure 8.** The comparison of methanol-to-propane retention time ratios for the various stationary phases provides a useful metric quantifying the relative polarity of each phase. By this metric the stationary phases have ratios of 89, 7, and 2 for HKUST-1, U-Bond PLOT, and PEG polymer, respectively.

## 4.5 Determining MOF Film Thickness from Chromatography

We previously mentioned that the partition coefficient as a function of temperature for HKUST-1 for several analytes was determined by employing experimental, chromatographic retention factors coupled with MOF film thicknesses measured using scanning electron microscopy (SEM). Now the partition coefficient is known for several analytes as a function of temperature, once and for all, and—of course—-independent of stationary-phase thickness (see [figure 7](#) and [table I](#)). Once the value of  $K$  is known it can be combined with retention factor data to back-calculate the HKUST-1 film thickness of a  $\mu$ GC column without resorting to destructive SEM imaging. The film thickness can then be correlated to the number of MOF LBL deposition cycles and enable tailoring of chromatographic performance. [Figure 9](#) is a plot of HKUST-1 film thickness as a function of the number of deposition cycles,  $N$ . Here we report two data points for the mean film thickness directly measured with SEM (blue squares). The mean thickness values for each column are derived from the average retention factor values measured at four temperatures for the four analytes: ethane, propane, *i*-butane, and *n*-butane. In other words, each  $d_f$  value plotted in [figure 9](#) represents 16 individual measurements across four temperatures and four analytes (a total of 112 data points for the seven measurements). [Figure 9](#) illustrates the remarkable agreement between SEM-measured and chromatographically determined  $d_f$  values above 17 depositions cycles ( $R^2 = 0.98$ ). Though we do not bear out a concrete proof here, this is indeed a good indication that these MOF films are behaving similarly to polymers with regard to their sorption thermodynamics (i.e. Flory-Huggins mass sorption models). A 10-deposition-cycle HKUST-1  $\mu$ GC column was also interrogated with SEM however incomplete surface coverage of the MOF film prevented reliable thickness measurements (a detail we will expound upon shortly). Yet the column is able to retain these light hydrocarbons to enable calculation of an *effective*—though not physically accurate—average, conformal-film thickness. This elicits the question; why isn't the film thickness linear in the number of cycles across the entire range?

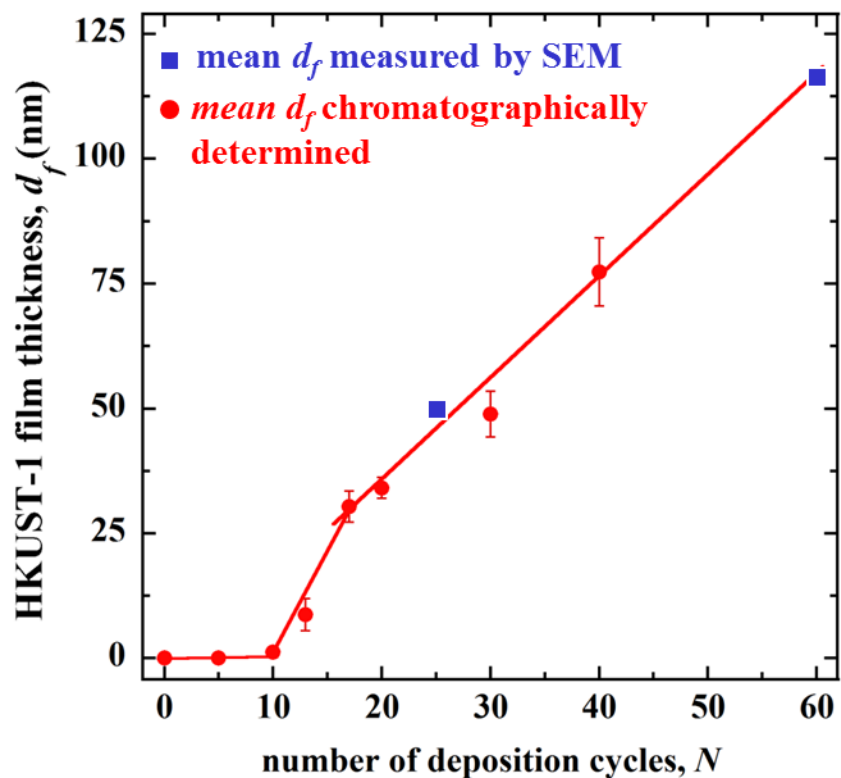


**Figure 9.** HKUST-1 film thickness deposited within  $\mu$ GC columns is plotted as a function of the number of deposition cycles. Here the blue squares represent thickness data determined by SEM microscopy, whereas the red data are calculated from known partition coefficients for several analytes and chromatographic retention time data ( $k$ ) to calculate a film thickness from Eq. 1&2. There is excellent agreement between the measured and calculated film thicknesses above 17 deposition cycles with an  $R^2 = 0.98$ .

## 4.6 Using Chromatography to Probe Layer-by-Layer Deposition Kinetics of SURMOF Thin Films on $\mu$ GC Column Channels

It is useful to look at these same data in [figure 9](#) instead in terms of *deposition rate* as a function of number of cycles as in [figure 10](#) below. In this plot the deposition rate is near zero until greater than five deposition cycles at which point the rate increases rapidly until  $\sim 17$  cycles. The deposition rate then reaches a steady-state value of 1.8 nm/cycle. Comparing the MOF film morphology for the three columns imaged by SEM ([figure 11a–c](#)) lends credence to a hypothesis that this non-constant deposition rate is a result of a nucleation phenomenon wherein the onset of complete conformal substrate coverage takes place at  $\sim 17$  cycles. The micrographs of 25 and 60 cycle MOF films show conformal films whereas that of 10-cycle column shows island-type growth. The two zoomed out images also show morphology changes of the spider web-like island chains. It stands to reason that these differences in morphology and coverage area could be caused by slight differences in the surface chemistry of the Bosch (DRIE)-etched, nominally hydroxylated SiO<sub>2</sub> channel walls. In [figure 12](#) it is evident that the HKUST-1 film coverage and morphology vary at different places (or heights) on a single channel wall itself. It should be noted that the deposition rate on a UV-ozone cleaned SiO<sub>2</sub> coated quartz crystal microbalance was at steady state immediately and rate actually decreased after  $\sim 20$  cycles (see previous [figure 4](#)). The decrease can be partially explained by the decrease in reaction rate of the trimesic acid where the data indicates that the time for complete reaction was not enough as the deposition proceeded. Although a thorough investigation into these observations is not within the scope of this research, these data and observations certainly point to the importance of surface preparation when depositing these MOF films.

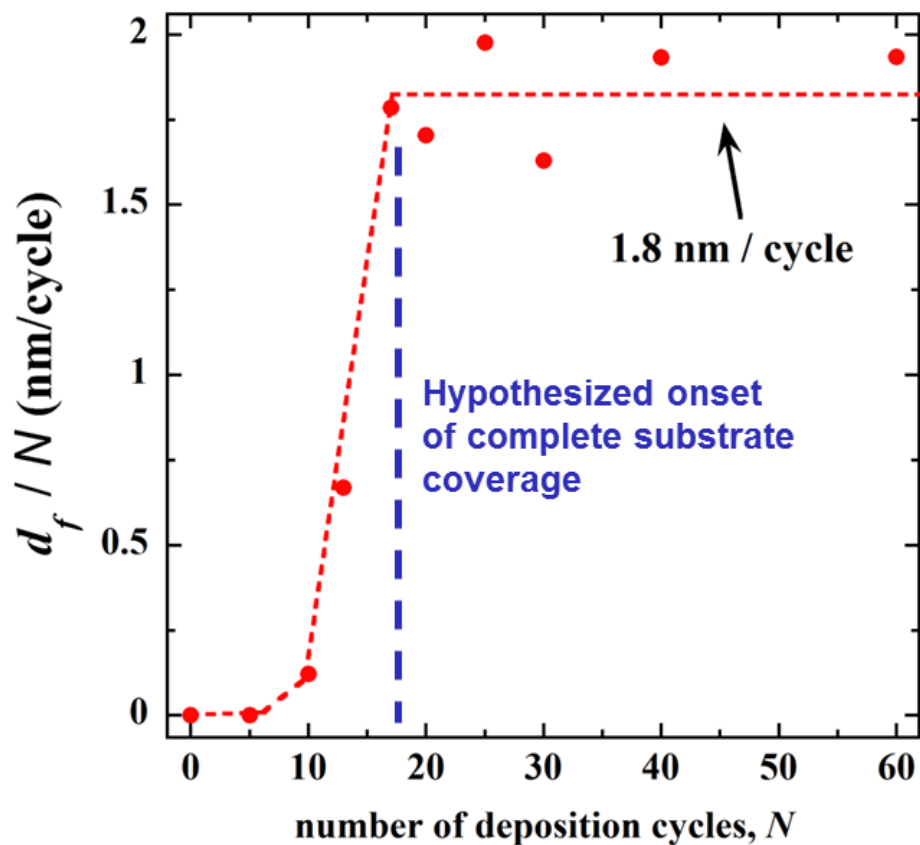


**Figure 10.** When the deposition rate of HKUST-1 films is plotted as a function of the number of deposition cycles it becomes very clear that the rate is near zero for the first several cycles until it rapidly climbs and reaches a steady-state value of 1.8nm /cycle after ~17 cycles. This is consistent with nucleation-dependent growth wherein a steady-state deposition rate would correspond to complete substrate coverage as shown in figure 11 below.

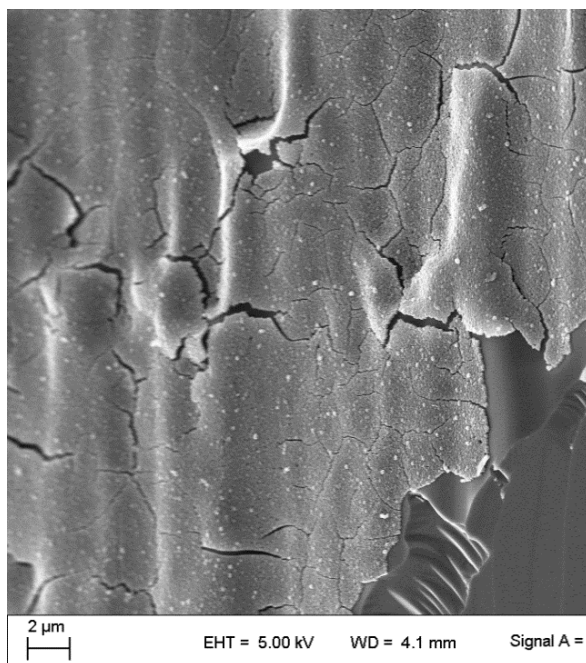
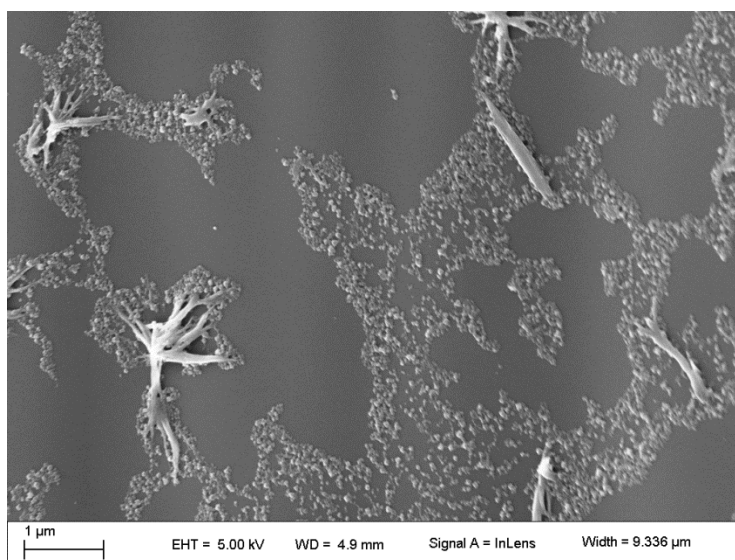


**Figure 11.** SEM micrographs of  $\mu\text{GC}$  columns coated with: **(a)** 10, **(b)** 25, and **(c)** 60 deposition cycles of HKUST-1 reveal that there are conformal thin films in the cases of 25 and 50 cycles, whereas for the 10-cycle column there is incomplete coverage (MOF islands/nucleation sites). Though the data is limited, the image for the 10-cycle column corroborates the thickness data calculated from chromatographic data.

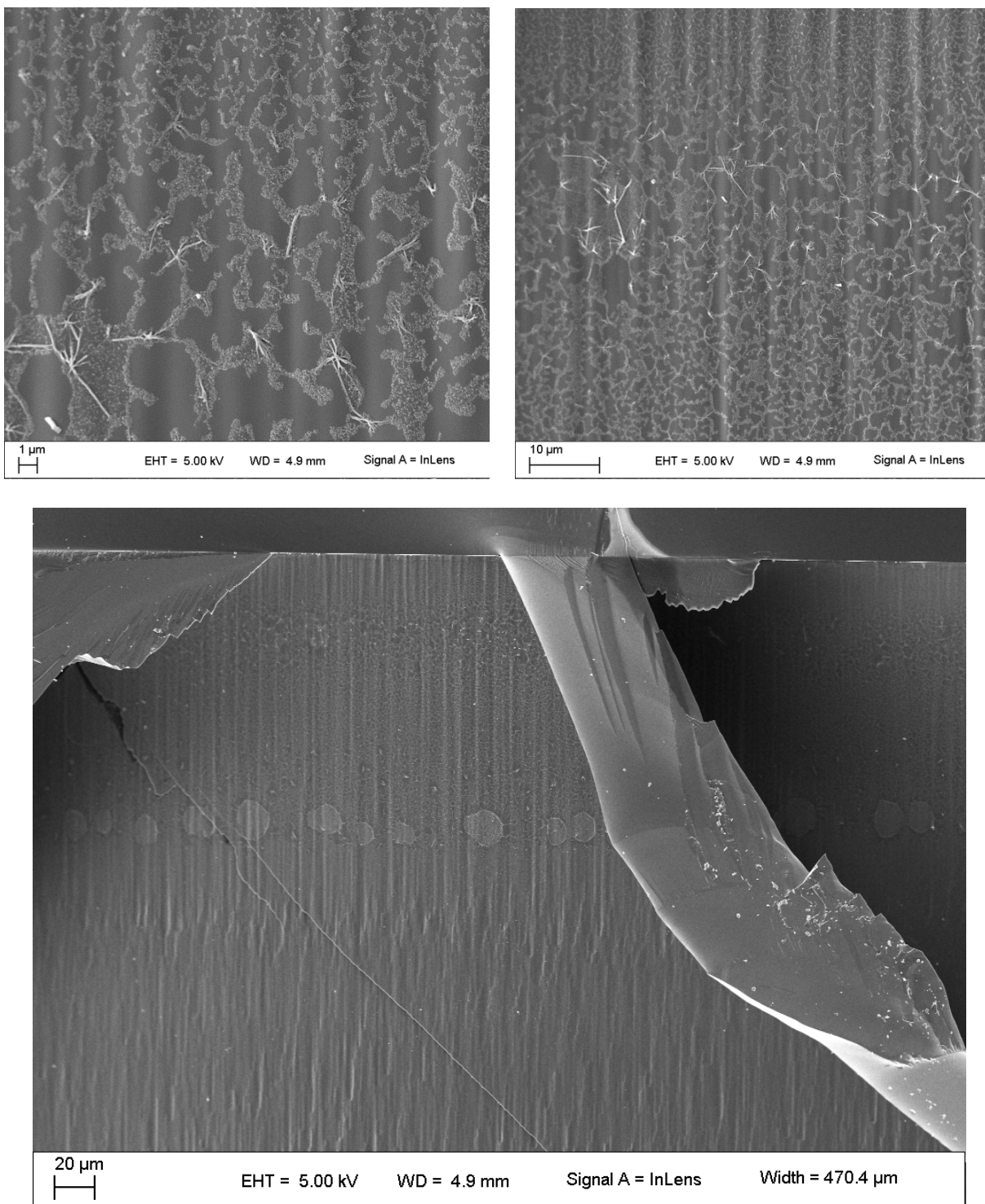


**Figure 12.** SEM micrographs of the 10-cycle HKUST-1  $\mu\text{GC}$  column channel wall at various magnification shows that film morphology and surface coverage vary even from the top to the bottom of the channel wall. Although the reason for this is not known, this phenomenon points to the possibility that even small discrepancies in surface chemistry could have a large effect on HKUST-1 film growth.

## 4.7 Determining Partition Coefficients for Toxic Industrial Chemicals and HKUST-1 Stationary Phases

Chromatographic experiments using actual TICs proved to be challenging for a number of reasons including: ensuring proper safety protocol for handling commercially purified TICs; the in-house availability of a detector with sufficient sensitivity; and impurity and concentration issues arising from *in situ* TIC gas generation (see experimental section). An example chromatographic separation of chlorine, chloromethane, and methylene chloride is shown below in figure 13. Although the detector signal to noise was very low for TICs, we were still able to determine the retention times for a  $\mu$ GC column with a known HKUST-1 film thickness. This allowed for the determination of the HKUST-1 partition coefficients at 50°C for the select TICs: chlorine, chloromethane, carbon disulfide, and methylene chloride. In figure 14 these TIC partition coefficients are compared to light hydrocarbons and it is shown that *K*-values range between those of ethane and propane. It is recommended that this work be continued with suitable detectors and purified analyte samples to fully characterize the chromatographic performance of these HKUST-1 films for these TICs.

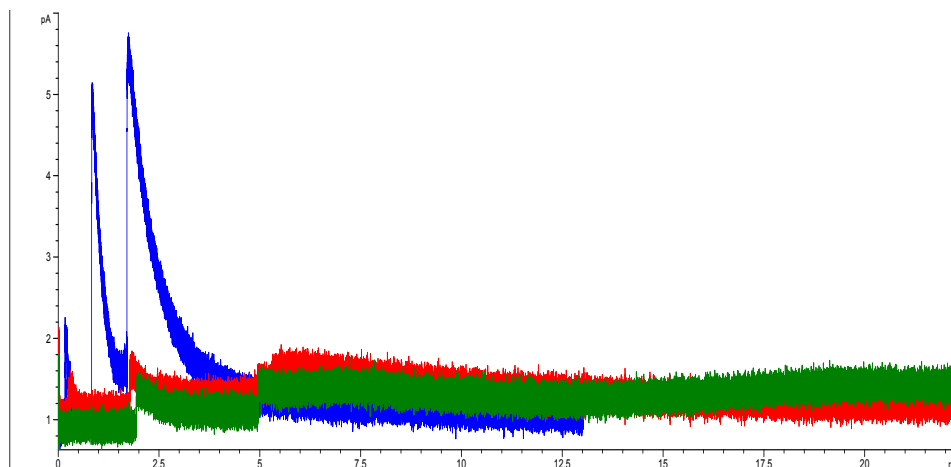


**Figure 13.** Total ion count chromatogram showing the separation of chlorine, chloromethane, and methylene chloride (blue trace) with a 20-cycle HKUST-1  $\mu$ GC column. GC conditions were as follows: 70°C isothermal, H<sub>2</sub> carrier gas at 5psi inlet pressure.

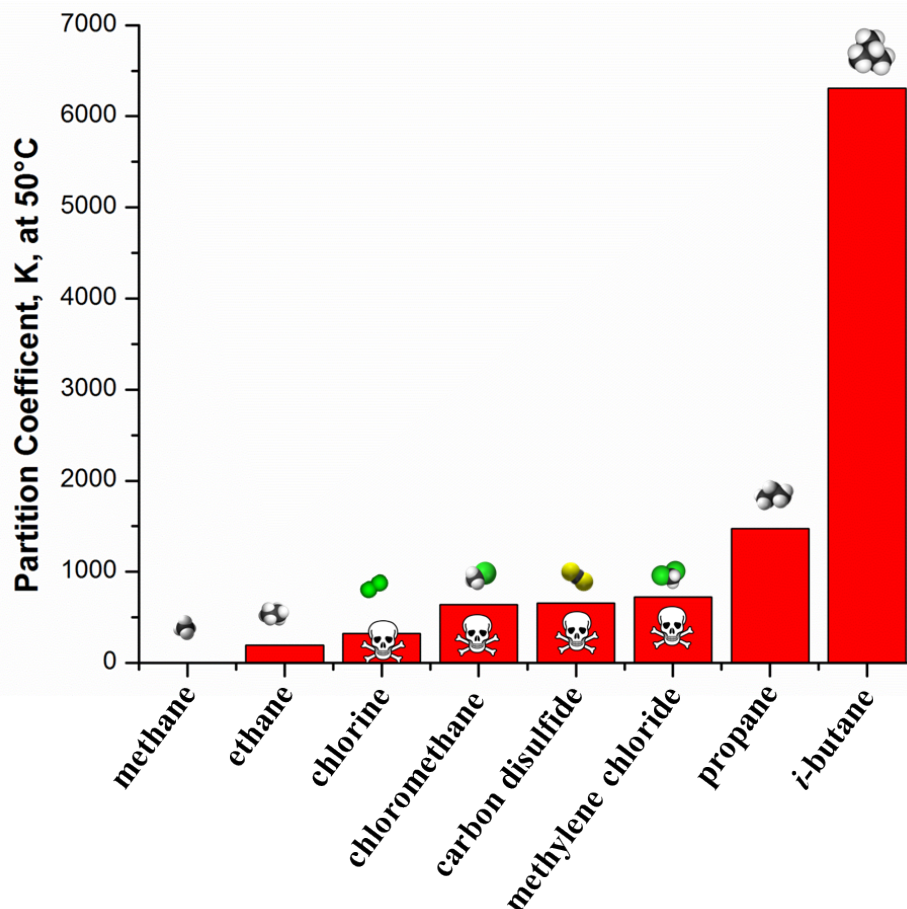


**Figure 14.** Partition coefficients at 50°C for HKUST-1 and select toxic industrial chemicals were determined from chromatographic retention time data and compared with those of light hydrocarbons. Here we see that these TICs have  $K$ -values that fall between those of ethane and pentane although lack of a suitable detector and pure analytical samples have made chromatographic characterization challenging.

#### 4.8 Novel Comprehensive $\mu\text{GC} \times \mu\text{GC}$ Using MOF Stationary Phases for the 2D Separation of Natural Gas

Comprehensive GC $\times$ GC is an analytical method by which two GC columns with disparate stationary phases are connected in series to yield 3-D chromatogram in a single analysis (i.e. a single sample injection). GC $\times$ GC relies on a modulation device to “inject” time-partitioned aliquots from the first column’s effluent onto the second column. Usually, column pairs are selected to have opposite polarity (i.e. hydrophobic and hydrophilic), though other orthogonal chemical interactions may be used. The modulation device can rely on either temperature or pressure to effect the modulation. Thermal modulation is discussed in detail by others.<sup>[11]</sup> Here we give a *brief* description of pressure-induced modulation, which is referred to as *stop-flow GC $\times$ GC*.<sup>[11]</sup> It is perhaps easiest to describe the technique schematically (figure 15 below). Here the two  $\mu\text{GC}$  columns and a solenoid valve are connected by a tee. The carrier gas is pressure regulated and flows into GC<sub>1</sub>. The solenoid valve leg is pressurized such that  $P_0$  and  $P_1$  are equal. In this case when the valve is open, pressure is equal at both the inlet and outlet of GC<sub>1</sub>, and no pressure gradient means that flow is stopped altogether through GC<sub>1</sub>. Simultaneously, flow is accelerated from the valve inlet through the GC<sub>2</sub> leg alone. When the

solenoid valve is closed the carrier gas flows out of GC<sub>1</sub> and into GC<sub>2</sub>. When the valve is modulated quickly (typically in fractions of a second), this process has the effect that can be described as taking a slice of GC<sub>1</sub> effluent and injecting that slice into the disparate GC<sub>2</sub> for a separate, orthogonal analysis. Analytes that have the same retention time on GC<sub>1</sub> (co-elution) will most likely be separated by the second column. The data from this single analysis is processed and represented as a 3-D plot where the x-axis and y-axis are the retention times on the first and second columns, respectively, and the z-axis is the detector amplitude. This extra dimension of separation from a single sample injection is especially useful for high-speed chromatography for which chromatographic efficiency and resolution are necessarily sacrificed for speed. Figure 16 displays a picture of an actual  $\mu$ GC  $\times$   $\mu$ GC device (without the detector and micro-column and valve inlet and outlet plumbing). In this same figure we show a picture of a commercial (Leco Inc.) GC $\times$ GC time-of-flight mass spectrometer to illustrate the difference in size.

Figure 17 a & b are  $\mu$ GC  $\times$   $\mu$ GC chromatograms (raw 2-d and processed 3-d chromatograms) for which a 70x685 $\mu$ m x120cm  $\mu$ GC column coated with HKUST-1 and a 30x685 $\mu$ m x30cm  $\mu$ GC column coated with ZIF-8 is used to separate natural gas (C1-C4). This represents the first ever  $\mu$ GC  $\times$   $\mu$ GC separation of permanent gases—in general—let alone with the use of disparate polarity MOF stationary phases. Figure 18 is a  $\mu$ GC  $\times$   $\mu$ GC chromatogram for which both long and short GC<sub>1</sub> and GC<sub>2</sub> columns are coated with HKUST-1 films. This is not as interesting from a separation-science perspective because using the same stationary phase for both columns in a GC $\times$ GC setup is not practically advantageous. However, the ZIF-8 thin films are not as well controlled/behaved as the HKUST-1 films and therefore do not yield as high a chromatographic resolution under the conditions used. So, the purpose of this chromatogram is to illustrate a higher resolution GC $\times$ GC chromatogram with more symmetric peaks than are possible with nonuniform ZIF-8 stationary phase films.

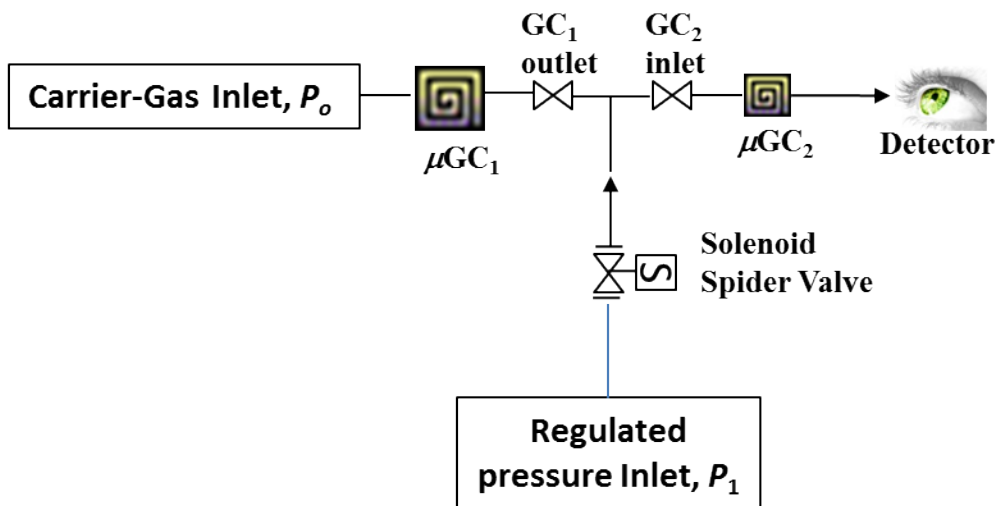
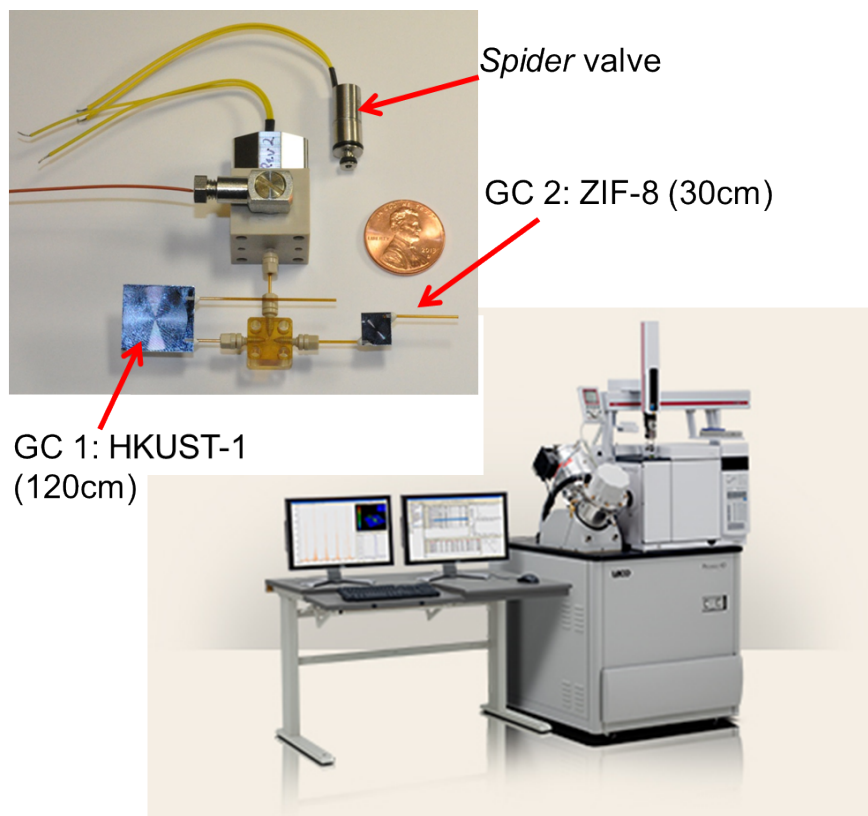
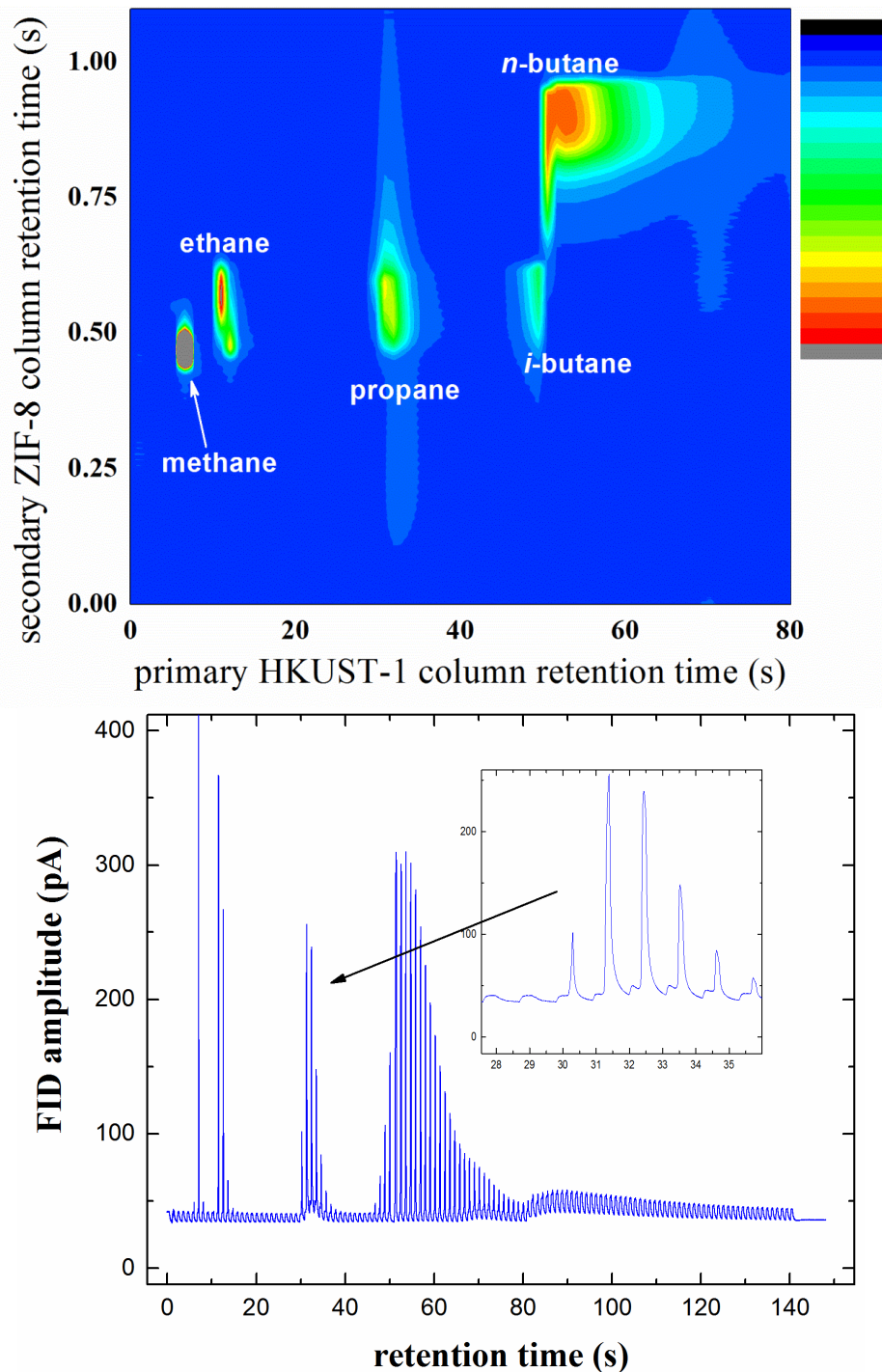


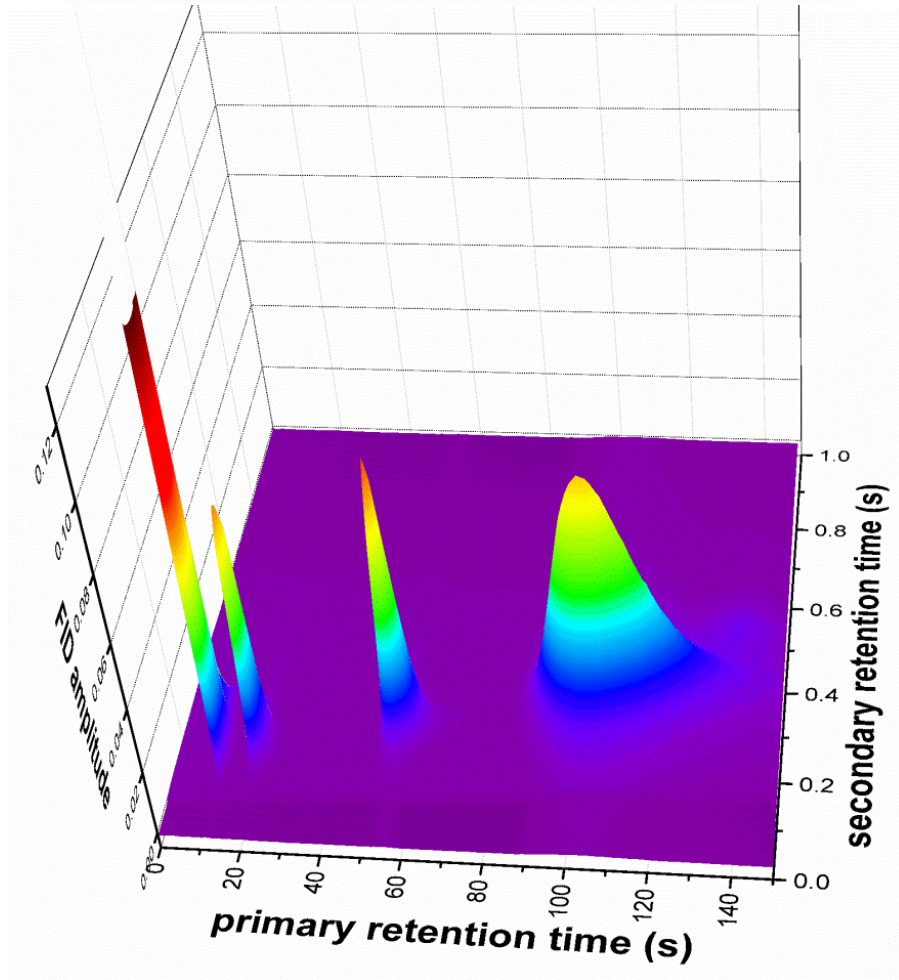
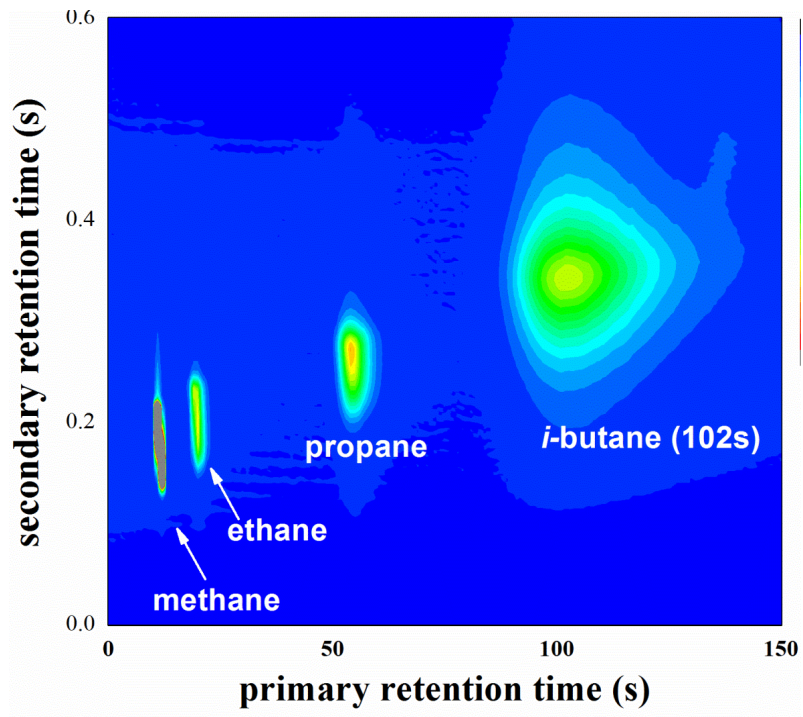
Figure 15. Schematic representation of a stop-flow, comprehensive GC $\times$ GC setup.



**Figure 16.** An actual picture of a  $\mu\text{GC} \times \mu\text{GC}$  device with a U.S. penny for scale (without the detector and micro-column and valve inlet and outlet plumbing). An additional *spider* solenoid valve is placed near the connected valve manifold for illustration purposes. In this same figure we show a picture of a commercial (Leco Inc.) GCxGC time-of-flight mass spectrometer to illustrate the difference in size.



**Figure 17.** (a) A contour (3-D) chromatogram showing the first reported  $\mu\text{GC} \times \mu\text{GC}$  separation of natural gas—in general—let alone using disparate MOF stationary phases. Here the stationary phases are HKUST-1 and ZIF-8. The normalized amplitude contour scale ranges from 0 to 0.12 (the methane peak is cut short for clarity). (b) These same data in (a) with no processing (i.e. detector amplitude as a function of time). Each individual slice (see inset figure) represents a separate second column chromatogram.



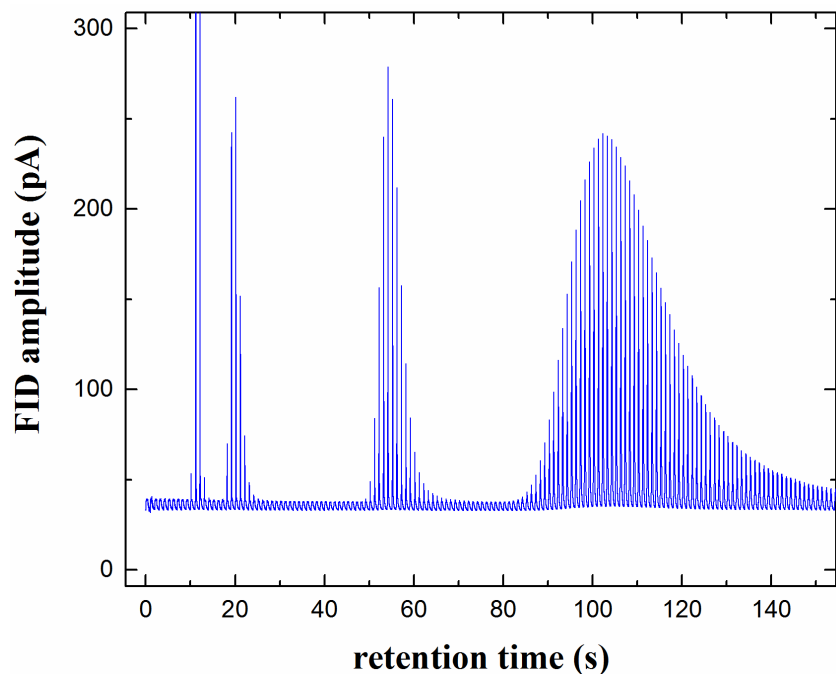


**Figure 18.** Chromatograms showing the  $\mu\text{GC} \times \mu\text{GC}$  separation of natural gas using  $\mu\text{GC}$  columns both coated with HKUST-1 stationary phases. Although using the same stationary phase in both columns is not very interesting from a separation science perspective, these chromatograms showcase the excellent resolution possible with well-behaved MOF stationary phase films. **(a)** 3-D contour  $\mu\text{GC} \times \mu\text{GC}$  chromatogram; **(b)** 3-D surface  $\mu\text{GC} \times \mu\text{GC}$  chromatogram; and **(c)** the raw kinetic amplitude data.

## 5. CONCLUSIONS

We have demonstrated the successful integration of MOF, thin-film stationary phases with Sandia's microfabricated gas chromatography columns. This was accomplished using layer-by-layer deposition techniques that allow for extraordinary control over MOF film thickness and chromatographic performance. We have demonstrated the first reported MOF-stationary-phase, high-speed chromatographic separation of natural gas using  $\mu$ GC columns—outperforming commercial stationary PLOT phases in terms of both polarity and absolute partition coefficients. The partition coefficients for HKUST-1 with light hydrocarbons and select TICs were determined, which led to a method for determining HKUST-1 film thickness from chromatography data alone. These data also suggest that MOFs behave similarly in terms of their sorption thermodynamics (as determined by chromatography) when compared to traditional polymer stationary phases, which is an unexpected result. When these thickness data were correlated to the number of deposition cycles and subsequently compared to MOF film coverage and morphology, we offered insight into the kinetics of HKUST-1 thin film growth within  $\mu$ GC column channels. These data lead to the hypothesis that HKUST-1 film growth on these surfaces is non-conformal until  $\sim 17$  deposition cycles at which point a steady-state deposition rate is achieved. In addition we have demonstrated the first reported  $\mu$ GC  $\times$   $\mu$ GC separation of natural gas—in general—let alone for two disparate MOF stationary phases. This research serves as a proof-of-concept for the use of these materials for portable light-molecule, chem-detection applications. Yet we have only scratched the surface of possibilities, due to the vast number of candidate MOF materials that could be employed. Future research could explore the phase space of available MOF materials with differing pore sizes, morphology and chemical functionality. Additionally, surface modifications (such as self-assembled monolayer coupling agents) could be used to improve MOF deposition.

## 6. REFERENCES

- [1] Lindner, D., “The  $\mu$ ChemLab<sup>TM</sup> project: micro total analysis system R&D at Sandia National Laboratories”, *Lab on a Chip*, 2001, 1, 15N-19N.
- [2] Lefebvre, D., Ricoul, F., Charleux, B., Thieuleux, C. “A Novel Stationary Phase for Light Alkanes Separation in Microfabricated Silicon Gas Chromatography Columns”, *Proceedings of the 17<sup>th</sup> International Conference on Miniaturized Systems for Chemistry and Life Sciences, October 2013, Freiburg Germany*.
- [3] Bétard, A., Fischer R.A., “Metal-Organic Framework Thin Films: From Fundamentals to Applications.”, *Chemical Reviews*. 2012, 112, 1055–1083.
- [4] Kreno, L.E., Leong, K., Farha, O.K., Allendorf, M., Van Duyne, R.P., Hupp, J.T., “Metal-Organic Framework Materials as Chemical Sensors”, *Chemical Reviews*, 2012, 112, 1105–1125.
- [5] Gu, Z.Y., Yan, X.P., “Metal-Organic Framework MIL-101 for High-Resolution Gas-Chromatographic Separation of Xylene Isomers and Ethylbenzene”, *Angew. Chem. Int. Ed.*, 2010, 49, 1477–1480.
- [6] Xie, S.M., Zhang, Z.J., Wang, Z.Y., Yuan, L.M., “Chiral Metal-Organic Frameworks for High-Resolution Gas Chromatographic Separations”, *J. Am. Chem. Soc.*, 2011, 133, 11892–11895.
- [7] Shekhah, O., Wang, H., Strunskus, T., Cyganik, P., Zacher, R., Wöll, C., *Langmuir*, 2007, 23, 7440-7442.
- [8] Shekhah, O., Wang, H., Kowarik, F., Schreiber, F., Paulus, M., Tolan, M., Sternemann, C., Evers, F., Zacher, D., Fischer, R.A., Wöll, C., *J. Am. Chem. Soc.*, 2007, 129, 15118-15119.
- [9] Stavila, V., Volponi, J., Katzenmeyer, A.M., Dixon, M.C., Allendorf, M.D., “Kinetics and mechanisms of metal-organic framework thin film growth: systematic investigation of HKUST-1 deposition on QCM electrodes”, *Chem. Sci.*, 2012, 3, 1531-1540.
- [10] Moorman, M.W., Manginell, R.P., Anderson, J.M., Simonson, R.J., Read, D.H., “Sealed Micro-Gas-Chromatography Columns and Methods Thereof”, Sandia National Laboratories, U.S. Patent Application Number 62105019, Attorney Reference Number SD-12950.0/S-132777
- [11] Libardoni, M., “Comprehensive Two-Dimensional Gas Chromatography (GCxGC)– Exploring its Effective Use as a Routine Analytical Technique”, Leco, Inc. presentation.

## 7. DISTRIBUTION

1	MS0963	Douglas Read	2718
1	MS1425	Colin Sillerud	1714
1	MS1425	Steven Casalnuovo	1714
1	MS0899	Technical Library	9536 (electronic copy)
1	MS0359	D. Chavez, LDRD Office	1911

